

Artificial Intelligence in *Cancer*

Artif Intell Cancer 2022 April 28; 3(2): 17-41



MINIREVIEWS

- 17 Usefulness of artificial intelligence in early gastric cancer
Panarese A

ORIGINAL ARTICLE**Basic Study**

- 27 Learning models for colorectal cancer signature reconstruction and classification in patients with chronic inflammatory bowel disease
Abaach M, Morilla I

ABOUT COVER

Editorial Board Member of *Artificial Intelligence in Cancer*, Maher a Sughayer, MD, Full Professor, Department of Pathology, King Hussein Cancer Center, Amman 11941, Jordan. msughayer@khcc.jo

AIMS AND SCOPE

The primary aim of *Artificial Intelligence in Cancer (AIC, Artif Intell Cancer)* is to provide scholars and readers from various fields of artificial intelligence in cancer with a platform to publish high-quality basic and clinical research articles and communicate their research findings online.

AIC mainly publishes articles reporting research results obtained in the field of artificial intelligence in cancer and covering a wide range of topics, including artificial intelligence in bone oncology, breast cancer, gastrointestinal cancer, genitourinary cancer, gynecological cancer, head and neck cancer, hematologic malignancy, lung cancer, lymphoma and myeloma, pediatric oncology, and urologic oncology.

INDEXING/ABSTRACTING

The *AIC* is now abstracted and indexed in Reference Citation Analysis, China Science and Technology Journal Database.

RESPONSIBLE EDITORS FOR THIS ISSUE

Production Editor: *Yu-Xi Chen*, Production Department Director: *Xu Guo*, Editorial Office Director: *Jin-Lei Wang*.

NAME OF JOURNAL

Artificial Intelligence in Cancer

ISSN

ISSN 2644-3228 (online)

LAUNCH DATE

June 28, 2020

FREQUENCY

Bimonthly

EDITORS-IN-CHIEF

Mujib Ullah, Cedric Coulouarn, Massoud Mirshahi

EDITORIAL BOARD MEMBERS

<https://www.wjgnet.com/2644-3228/editorialboard.htm>

PUBLICATION DATE

April 28, 2022

COPYRIGHT

© 2022 Baishideng Publishing Group Inc

INSTRUCTIONS TO AUTHORS

<https://www.wjgnet.com/bpg/gerinfo/204>

GUIDELINES FOR ETHICS DOCUMENTS

<https://www.wjgnet.com/bpg/GerInfo/287>

GUIDELINES FOR NON-NATIVE SPEAKERS OF ENGLISH

<https://www.wjgnet.com/bpg/gerinfo/240>

PUBLICATION ETHICS

<https://www.wjgnet.com/bpg/GerInfo/288>

PUBLICATION MISCONDUCT

<https://www.wjgnet.com/bpg/gerinfo/208>

ARTICLE PROCESSING CHARGE

<https://www.wjgnet.com/bpg/gerinfo/242>

STEPS FOR SUBMITTING MANUSCRIPTS

<https://www.wjgnet.com/bpg/GerInfo/239>

ONLINE SUBMISSION

<https://www.f6publishing.com>



Usefulness of artificial intelligence in early gastric cancer

Alba Panarese

Specialty type: Gastroenterology and hepatology

Provenance and peer review: Invited article; Externally peer reviewed.

Peer-review model: Single blind

Peer-review report's scientific quality classification

Grade A (Excellent): 0
Grade B (Very good): 0
Grade C (Good): C, C, C, C
Grade D (Fair): 0
Grade E (Poor): 0

P-Reviewer: Cheng H, China; Kawabata H, Japan; Luo W, China; Yu W, China

Received: December 31, 2021

Peer-review started: December 31, 2021

First decision: March 12, 2022

Revised: March 27, 2022

Accepted: April 20, 2022

Article in press: April 20, 2022

Published online: April 28, 2022



Alba Panarese, Department of Gastroenterology and Endoscopy, Central Hospital, Taranto 74123, Italy

Corresponding author: Alba Panarese, MD, Director, Department of Gastroenterology and Endoscopy, Central Hospital, Bruno Street, 1, Taranto 74123, Italy. albapanarese@libero.it

Abstract

Gastric cancer (GC) is a major cancer worldwide, with high mortality and morbidity. Endoscopy, important for the early detection of GC, requires trained skills, high-quality technologies, surveillance and screening programs. Early diagnosis allows a better prognosis, through surgical or curative endoscopic therapy. Magnified endoscopy with virtual chromoendoscopy remarkably improve the detection of early gastric cancer (EGC) when endoscopy is performed by expert endoscopists. Artificial intelligence (AI) has also been introduced to GC diagnostics to increase diagnostic efficiency. AI improves the early detection of gastric lesions because it supports the non-expert and experienced endoscopist in defining the margins of the tumor and the depth of infiltration. AI increases the detection rate of EGC, reduces the rate of missing tumors, and characterizes EGCs, allowing clinicians to make the best therapeutic decision, that is, one that ensures curability. AI has had a remarkable evolution in medicine in recent years, moving from the research phase to clinical practice. In addition, the diagnosis of GC has markedly progressed. We predict that AI will allow great evolution in the diagnosis and treatment of EGC by overcoming the variability in performance that is currently a limitation of chromoendoscopy.

Key Words: Early gastric cancer; Artificial intelligence; *Helicobacter pylori*; Endoscopic submucosal dissection; Dysplasia; Computer-aided; Detection

©The Author(s) 2022. Published by Baishideng Publishing Group Inc. All rights reserved.

Core Tip: Early diagnosis and treatment of gastric cancer (GC) can benefit from the introduction of artificial intelligence (AI) into endoscopic diagnostics of the upper digestive tract. AI improves endoscopic diagnosis because it overcomes the difficulty of diagnosis linked to the experience of the endoscopist. Improving endoscopic diagnosis will allow for better treatment, which is more likely to be curative, with submucosal endoscopic dissection or surgery. However, because research advances in this area continue to be rapid, prospective multicenter studies are needed on the application of AI to the diagnosis of early GC.

Citation: Panarese A. Usefulness of artificial intelligence in early gastric cancer. *Artif Intell Cancer* 2022; 3(2): 17-26

URL: <https://www.wjgnet.com/2644-3228/full/v3/i2/17.htm>

DOI: <https://dx.doi.org/10.35713/aic.v3.i2.17>

THE RELEVANCE DIAGNOSIS OF GASTRIC CANCER

Gastric cancer (GC), the fourth leading cause of cancer in men and seventh in women, is still third for cancer-related deaths worldwide[1]. It's 5-year survival rate is less than 40%[2] and its prognosis is related to the stage at the time of detection. The 5-year survival rate of patients with early gastric cancer (EGC) is 91.5%, whereas it is 16.4% for patients in the advanced stage[2-4]. The screening programs are cost effective in high-incidence regions[1,5] and advanced endoscopic technologies allow endoscopists to diagnose EGC[6-8]; however, optical diagnosis requires a period of training[9].

Recently, the practice of medicine has changed with the development of artificial intelligence (AI) based on image recognition with deep learning (DL) using the convolutional neural network (CNN), which, in upper endoscopy, is trained with endoscopic images and detects GC accurately[10-14]. Several AI-assisted CNN computer-aided diagnosis (CAD) systems have been built, with diagnostic precision in the detection of GC based on different types of endoscopic images. AI helps endoscopists to achieve the accuracy needed for GC screening, surveillance of precancerous, as well as for detecting the depth of invasion of gastric lesions, and when applied to radiological imaging techniques, lymph node and peritoneal metastasis[11-14].

OPTICAL ENDOSCOPIC DIAGNOSIS OF EGC

While computed tomography, endoscopic ultrasound, and positron emission tomography are important for the diagnosis and staging of advanced GC, endoscopy plays an essential role in the early detection of EGC, as it allows the gastric mucosa to be examined directly. Endoscopy with targeted biopsies is the gold standard method for diagnosing EGC, and the accurate diagnosis of EGC through endoscopic imaging is a primary goal for improving the poor prognosis of patients[4,15-17]. Although the quality and accuracy of endoscopic detection are variable between centers and endoscopists, endoscopy is crucial because many early-stage tumors (*i.e.* intramucosal cancer) can be resected endoscopically in a curative manner, with an excellent prognosis at 5 years[4,18,19].

Unfortunately, few endoscopists are experts in advanced endoscopic imaging, and diagnostic accuracy depends largely on the clinical experience of the experts and is influenced by multiple factors, such as training and technologies[9,20]. Ultimately, early diagnosis and curative treatment are important for prognosis but can be difficult to achieve depending on the endoscopist[10,21]. The false negative rate of GC detected by esophagogastroduodenoscopy is 4.6-25.8[22-24], with higher values for inexperienced endoscopists[9,25]. The diagnostic capacity of endoscopists, due to the endoscopic appearance of EGC, which is usually very subtle, varies widely with regard to the differentiation between GC and gastritis, the prediction of the horizontal extension of GC and the depth of invasion [26].

As lesions of the gastric mucosa develop according to the Correa cascade, from atrophy to intestinal metaplasia, intraepithelial neoplasia and invasive neoplasia[27,28]; improving the accuracy of endoscopic diagnosis of precancerous lesions and EGC through screening and surveillance programs, is useful to reduce the incidence and mortality of GC[29-31]. The standard modality for the detection of EGC is endoscopy with white light imaging (WLI), but its overall sensitivity is not satisfactory (40%-60%)[32]. Magnified endoscopy (ME) with image-enhanced endoscopy techniques such as narrow-band imaging (NBI; Olympus Co., Tokyo, Japan), flexible spectral imaging color enhancement (FICE; Fujifilm Co., Tokyo, Japan), and blue laser imaging (BLI; Fujifilm), improve the accuracy of the detection of gastric lesions[26,33,34]. In particular, ME-NBI, the most frequent technology used in AI studies, achieves significantly better sensitivity, specificity, and accuracy than WLI, facilitating examination of the glandular epithelium in the stomach by observing the microvascular architecture and structure of the microsurface[32,35-39].

However, the virtual chromoendoscopic diagnosis of EGC requires considerable skill and experience [9,38,40,41]. The diagnostic effectiveness of endoscopists non yet trained in differentiating EGC from non-cancerous lesions with ME-NBI is disappointing[9,36,41]. Optical diagnosis can improve with AI-assisted CNN, which has been mainly applied to ME-NBI[14].

AI FOR THE DIAGNOSIS OF EGC

AI, which mimics human cognitive function[42] with its efficient computational power and learning capabilities, can be applied to GC because it processes and analyzes large amounts of data with systems that classify and recognize lesion images without the need to write complicated image processing algorithms[43]. Therefore, AI could help gastroenterologists in clinical diagnosis and decision-making. Technically, the DL method approximates complex information using a multilayer system (*e.g.*, CNN), in which neural layers connect only to the next layer (Figure 1), overcoming the limitation of the "black box" of previous systems because it shows the reasons for the decisions made[44]. Over the years, new CNN-based systems have been introduced to analyze lesions of the gastric mucosa, using higher quality images and image selection strategies based on evidence from previous experiences. CNN systems in the initial training phase take a few hours to generate the identification system, which can then be used repeatedly; and has a good adaptability as it can be used on multiple platforms for the real-time analysis of JPEG images or video captured by chromoendoscopy. Magnifying chromoendoscopic images can improve the speed and accuracy of CNN diagnostics compared to conventional endoscopy alone[45, 46]. Typically, training images are judged by experienced endoscopists and pathologically confirmed, and only endoscopic and chromoendoscopic images with appropriate magnification and typical manifestation for learning the CNN model are selected.

In recent studies, other important outcomes have been added to the main outcome to establish endoscopic resectability, namely the identification of the margins and depth of the lesion[47-49]. Gastric tumors of differentiated intramucous type (m) or infiltrating only the superficial layer of the submucosal ($\leq 500 \mu\text{m}$: Sm¹) can be resected endoscopically, while those that deeply invade the submucosal ($> 500 \mu\text{m}$: Sm²) are surgically resected because of the risk of lymph node and distant metastases. The optical differentiation between m/Sm¹ and Sm² is often difficult[19].

Using PubMed, Embase, Web of Science, and Cochrane Library databases to search the literature on CAD systems for the diagnosis of EGC, we identified 26 relevant physician-initiated studies through November 2021. Table 1 summarizes the main characteristics of the studies (two single-center prospective[50,51], two multicenter prospective[49,52], and twenty-two retrospective[14,45-48,53-69]): Study design; endoscopic modality; main study aim; and subjects/lesions/images for validation. Table 2 describes the endpoints of the studies.

Selected studies included a diagnostic test on the application of AI in endoscopy for the diagnosis of EGC; the absolute numbers of true-positive, false-negative, true-negative and false-positive; clear information about data and number of images; the description of the algorithms and the process applied to the EGC diagnosis.

To form a training dataset, 11 studies used only WLI images[47,50-53,55-58,60,61], 9 only virtual chromoendoscopy images[48-49,59,63-68], 1 only WLI and chromoendoscopy images[54], and 5 WLI, chromoendoscopy and NBI images[14,45,46,62,69]. The identified studies were largely published in the last 3 years.

Overall, current CNN systems work quite well in detecting the endoscopic/chromoendoscopic characteristics of EGC and other gastric lesions and could provide diagnostic support to experienced and non-expert endoscopists in future practice. AI-assisted CNN CAD systems can avoid subjectivity during the processing and diagnosis of endoscopic/chromoendoscopic images; moreover, in the screening of GC, they work as a "confirmer" or "corrector," providing a second opinion to reduce the diagnostic errors committed by endoscopists and suggesting optimal treatment. Current studies by Asian authors[54,59] confirm that CAD systems detect EGCs and estimate the depth of infiltration and extension, overcoming the problem of operator training and the subjectivity of diagnosis. Moreover, if the first studies report comparable results between experts and CAD systems, the most recent ones show that AI has reached a sensitivity even higher than that of experts, with similar specificity[46]. Over time, images used for CAD system training have improved and, at present, advanced training strategies and videos are being used.

Namikawa *et al*[58] first reported the usefulness of AI systems in GC detection, developing the "original convolutional neural network (O-CNN)," with a relatively low positive predictive value (PPV). The same authors developed an advanced AI-based diagnostic system, "advanced CNN (A-CNN)", by adding a new training dataset to the O-CNN and evaluated its applicability for the classification of GC and gastric ulcer. The diagnostic performance of A-CNN was evaluated retrospectively using an independent validation dataset and compared to that of the O-CNN by estimating the overall accuracy of the classification. The sensitivity, specificity, and PPV rates of A-CNN for the classification of GC at the lesion level were 99.0%, 93.3%, and 92.5%, respectively, and 93.3%, 99.0%, and 99.1% for the classification of gastric ulcers. The overall accuracy of O-CNN and A-CNN in the classification of GC

Table 1 Studies involving computer-aided diagnosis for early gastric cancer detection

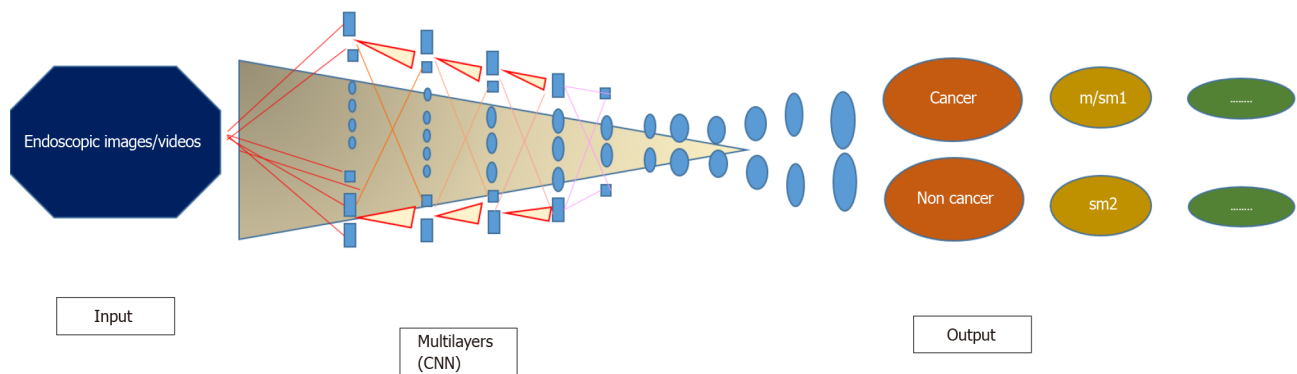
Ref.	Study design	Endoscopic modality	Main study aim	Subjects for validation
Kubota <i>et al</i> [53], 2012	Retrospective	WLI	Prediction of invasion depth	344 patients
Miyaki <i>et al</i> [63], 2013	Retrospective	ME-FICE	Differentiation of cancerous areas from non-cancerous areas	46 patients
Miyaki <i>et al</i> [64], 2015	Retrospective	ME-BLI	Differentiation of cancerous areas from non-cancerous areas	95 patients
Kanesaka <i>et al</i> [65], 2018	Retrospective	ME-NBI	Delineation of cancerous areas	81 images
Hirasawa <i>et al</i> [14], 2018	Retrospective	WLI, CE, NBI	Delineation of cancer	69 patients
Zhu <i>et al</i> [54], 2019	Retrospective	WLI, NBI	Prediction of invasion depth	203 lesions
Cho <i>et al</i> [50], 2019	Prospective validation dataset	WLI	Differentiation of cancerous areas from non-cancerous areas	200 patients
Ishioka <i>et al</i> [55], 2019	Retrospective	WLI	Detection of GC	62 patients
Yoon <i>et al</i> [56], 2019	Retrospective	WLI	Detection of GC	800 patients
Tang <i>et al</i> [57], 2020	Retrospective	WLI	Differentiation of cancerous areas from non-cancerous areas	279 patients
Namikawa <i>et al</i> [58], 2020	Retrospective	WLI	Differentiation of cancerous areas from non-cancerous areas	220 lesions
Li <i>et al</i> [66], 2020	Retrospective	ME-NBI	Detection of cancer	341 images
An <i>et al</i> [62], 2020	Retrospective	WLI, CE, ME-NBI	Delineation of EGC margins	355 images
Horiuki <i>et al</i> [67], 2020	Retrospective	ME-NBI	Differentiation of cancerous areas from non-cancerous areas	258 images
Nagao <i>et al</i> [45], 2020	Retrospective	WLI, CE, NBI	Prediction of invasion depth of GC	1084 GC
Wu <i>et al</i> [52], 2021	Prospective	WLI	Detection of Blind spots And early gastric cancer	1050 patients
Ueyama <i>et al</i> [59], 2021	Retrospective	ME-NBI	Differentiation of cancerous areas from non-cancerous areas	2300 images
Ling <i>et al</i> [48], 2021	Retrospective	ME-NBI	Differentiation status and margins for EGC	139 + 58 + 87 EGCs
Ikenoyama <i>et al</i> [46], 2021	Retrospective	WLI, CE, NBI	Detection of cancer	140 lesions
Hu <i>et al</i> [68], 2021	Retrospective	ME-NBI	Detection of cancer	295 lesions
Oura <i>et al</i> [60], 2021	Retrospective	WLI	Missing GC and point out low-quality images	855 lesions + 50 lesions
Zhang <i>et al</i> [61], 2021	Retrospective	WLI	Detection of cancer	1091 images
Wu <i>et al</i> [51], 2021	Prospective	WLI	Screening gastric lesions	10000 patients
Hamada <i>et al</i> [69], 2022	Retrospective	WLI, CE, BLI	Depth of invasion of EGC	68 patients
Nam <i>et al</i> [47], 2022	Retrospective	WLI	Lesion detection, differentiation and depth	1366 patients
Wu <i>et al</i> [49], 2022	Prospective	ME-NBI	GC and EGC detection, EGC invasion depth and differentiation status	

BLI: Blue laser imaging; CE: Color enhancement; EGC: Early gastric cancer; ME-NBI: Magnification endoscopy; NBI: Narrow-band imaging; WLI: White light imaging.

and gastric ulcer was 45.9% (GC: 100%, gastric ulcer 0.8%) and 95.9% (GC: 99.0%, gastric ulcer 93.3%), respectively, at the lesion level. The A-CNN system can effectively classify GC and gastric ulcer. Yu *et al* [36] explored the diagnostic capacity of the CNN system with ME-NBI to distinguish EGC from gastritis. CNN accuracy with ME-NBI images was 85.3% (220 of 258 images correctly diagnosed). Rates of sensitivity, specificity, PPV, and negative predictive value (NPV) were 95.4%, 71.0%, 82.3%, and 91.7%, respectively. In total, 7 of 151 EGC images were identified as gastritis, while 31 of the 107 gastritis images were recognized as EGC. The overall test speed was 51.83 images/s (0.02 s/image). CNN with

Table 2 Endpoints of the extracted studies

Ref.	Main outcome
[45,53,54,69]	Accuracy rate of diagnosing the depth of wall invasion of gastric cancer
[64]	Detection rate of gastric cancer
[63]	Identification rate of cancerous lesions, reddened lesions and surrounding tissue
[48,62,65]	Detection rate of early gastric cancer and its margins
[14]	Identification rate of gastric cancer and gastric ulcer
[50]	Identification rate of advanced gastric cancer, early gastric cancer, high grade dysplasia, low grade dysplasia and non-neoplasm
[46,51,55,57,59,60,66,68]	Detection rate of early gastric cancer
[56]	Detection rate of early gastric cancer and its localization. Accuracy rate of diagnosing the depth of wall invasion of gastric cancer
[58]	Identification rate of early gastric cancer, advanced gastric cancer and benign gastric ulcer
[67]	Identification rate of early gastric cancer and gastritis
[52]	Identification rate of early gastric cancer and number of blind spots
[61]	Identification rate of early gastric cancer and other gastric lesions (high grade dysplasia, peptic ulcer, advanced gastric cancer, gastric submucosal tumors and normal gastric mucosa)
[47]	Identification rate of early gastric cancer, advanced gastric cancer and benign gastric ulcer. Accuracy rate of diagnosing the depth of wall invasion of gastric cancer
[49]	Detection rate of early gastric cancer. Accuracy rate of diagnosing the depth of wall invasion of gastric cancer



DOI: 10.35713/aic.v3.i2.17 Copyright ©The Author(s) 2022.

Figure 1 The multilayer system in the diagnosis of early gastric cancer.

ME-NBI can differentiate between EGC and gastritis with high sensitivity and NPV in a short period of time. Thus, the A-CNN system can complement current clinical practice of diagnosis with ME-NBI.

Nam *et al*[47] have developed and validated CNN-based AI models for lesion detection, differential diagnosis (AI-DDx), and depth of invasion (AI-ID; pT1a *vs* pT1b among EGC). AI-DDx is comparable to experts and outperforms novice and intermediate endoscopists in the differential diagnosis of gastric mucosal lesions. AI-ID performs better than endoscopic ultrasound to assess depth of invasion. Ling *et al*[48] have developed a system to identify in real time with precision with ME-NBI the state of differentiation and delineate the margins of the EGC, fundamental to determine a surgical strategy and achieve the curative resection. In the unprocessed videos of EGC, the system obtained a real-time diagnosis of EGC differentiation and its margins ME-NBI endoscopy. This system has achieved higher performance than experts and has been successfully tested in real EGC videos.

Zhu *et al*[54] represented a further step forward because they developed an algorithm capable of differentiating lesions with Sm² invasion depth from m/Sm¹. AI has presented 76% sensitivity and 96% specificity in identifying “Sm² or deeper” cancers, resulting in significantly higher sensitivity and specificity than those achieved through visual inspection of endoscopists. The specificity of 96% could minimize the overdiagnosis of invasion, which would contribute to a reduction of unnecessary surgeries for m/Sm¹ cancers.

Wu *et al*[52], in a prospective multicenter randomized controlled trial, developed a CNN system to monitor blind spots during esophagogastroduodenoscopy, updating the previous system

(ENDOANGEL), verifying efficacy in improving endoscopy quality, and pretesting performance in detecting EGC.

Ultimately, AI is even superior to endoscopists experienced in identifying and classifying ECC, eliminates interobserver variability, and can train inexperienced endoscopists. Yet, it must optimize the ability to recognize all lesions (PPV) and not interpret the inflammatory or benign aspects of the mucosa as neoplastic (NPV). Over time, CAD systems have improved image selection strategies with strict criteria, using high-quality data and videos, and eliminating overlearning and misdiagnosis. Videos improve the performance of AI[55] because they represent real-life scenarios, and compared to static images improve PPV and NPV. Regarding the selection of images, gastritis, that is, the presence of inflammation, reduces the performance of AI[14] and endoscopists[70]. The small (diameter ≤ 5 mm) and depressed EGCs, difficult to distinguish from gastritis even for experienced endoscopists, influence the rate of false negatives; and gastritis with redness, atrophy and intestinal metaplasia affects the rate of false positives. In dedicated studies, CAD systems detect *Helicobacter pylori* (*H. pylori*) infection (sensitivity 89%, specificity 87% and diagnostic time 194 s)[71,72], but, regarding the diagnosis of EGC with AI systems, we propose to evaluate the gastric mucosa after the eradication of *H. pylori* to reduce the intensity of redness of gastritis.

Integrating in appropriate algorithms, through the intersection of engineering and medical expertise, high-quality image sets, poor images, and images from regular sites, will increase clinical effectiveness. Moreover, the products obtained through collaboration among centers specialized in the diagnosis and treatment of gastric lesions are reproducible and the limitation in applying AI to the diagnosis of EGC is the acquisition of new technologies, which requires investment. Finally, prospective multicenter trials are needed.

CONCLUSION

The application of AI to the clinical practice of the upper digestive tract increases the rate of EGC compared to all GCs, exceeding the subjectivity of the diagnosis and reducing the chance of missing EGCs. AI recognizes those lesions that not even the most experienced endoscopists can detect, as if “illuminating” the images with its third artificial eye. Of course, AI increases the accuracy of endoscopic diagnosis of EGC, especially when combined with the experience of endoscopists. However, since its introduction in this field is very recent, the results in clinical practice must be further validated, considering all possible aspects, both technical and technological concerning endoscopy, and organizational ones.

FOOTNOTES

Author contributions: Panarese A conceived, designed, wrote, and revised the manuscript.

Conflict-of-interest statement: There is no conflict of interest associated with the author.

Open-Access: This article is an open-access article that was selected by an in-house editor and fully peer-reviewed by external reviewers. It is distributed in accordance with the Creative Commons Attribution NonCommercial (CC BY-NC 4.0) license, which permits others to distribute, remix, adapt, build upon this work non-commercially, and license their derivative works on different terms, provided the original work is properly cited and the use is non-commercial. See: <https://creativecommons.org/licenses/by-nc/4.0/>

Country/Territory of origin: Italy

ORCID number: Alba Panarese 0000-0002-6931-2171.

S-Editor: Liu JH

L-Editor: A

P-Editor: Liu JH

REFERENCES

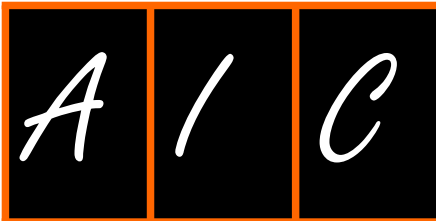
- 1 Ferlay J, Colombet M, Soerjomataram I, Mathers C, Parkin DM, Piñeros M, Znaor A, Bray F. Estimating the global cancer incidence and mortality in 2018: GLOBOCAN sources and methods. *Int J Cancer* 2019; **144**: 1941-1953 [PMID: 30350310 DOI: 10.1002/ijc.31937]
- 2 Song Z, Wu Y, Yang J, Yang D, Fang X. Progress in the treatment of advanced gastric cancer. *Tumour Biol* 2017; **39**: 1010428317714626 [PMID: 28671042 DOI: 10.1177/1010428317714626]
- 3 Nishizawa T, Yahagi N. Long-Term Outcomes of Using Endoscopic Submucosal Dissection to Treat Early Gastric Cancer.

- Gut Liver* 2018; **12**: 119-124 [PMID: 28673068 DOI: 10.5009/gnl17095]
- 4 **Young E**, Philpott H, Singh R. Endoscopic diagnosis and treatment of gastric dysplasia and early cancer: Current evidence and what the future may hold. *World J Gastroenterol* 2021; **27**: 5126-5151 [PMID: 34497440 DOI: 10.3748/wjg.v27.i31.5126]
 - 5 **Zhang X**, Li M, Chen S, Hu J, Guo Q, Liu R, Zheng H, Jin Z, Yuan Y, Xi Y, Hua B. Endoscopic Screening in Asian Countries Is Associated With Reduced Gastric Cancer Mortality: A Meta-analysis and Systematic Review. *Gastroenterology* 2018; **155**: 347-354.e9 [PMID: 29723507 DOI: 10.1053/j.gastro.2018.04.026]
 - 6 **Yao K**, Takaki Y, Matsui T, Iwashita A, Anagnostopoulos GK, Kaye P, Rangunath K. Clinical application of magnification endoscopy and narrow-band imaging in the upper gastrointestinal tract: new imaging techniques for detecting and characterizing gastrointestinal neoplasia. *Gastrointest Endosc Clin N Am* 2008; **18**: 415-433, vii [PMID: 18674694 DOI: 10.1016/j.giec.2008.05.011]
 - 7 **Osawa H**, Yamamoto H, Miura Y, Yoshizawa M, Sunada K, Satoh K, Sugano K. Diagnosis of extent of early gastric cancer using flexible spectral imaging color enhancement. *World J Gastrointest Endosc* 2012; **4**: 356-361 [PMID: 22912909 DOI: 10.4253/wjge.v4.i8.356]
 - 8 **Kimura-Tsuchiya R**, Dohi O, Fujita Y, Yagi N, Majima A, Horii Y, Kitaichi T, Onozawa Y, Suzuki K, Tomie A, Okayama T, Yoshida N, Kamada K, Katada K, Uchiyama K, Ishikawa T, Takagi T, Handa O, Konishi H, Kishimoto M, Naito Y, Yanagisawa A, Itoh Y. Magnifying Endoscopy with Blue Laser Imaging Improves the Microstructure Visualization in Early Gastric Cancer: Comparison of Magnifying Endoscopy with Narrow-Band Imaging. *Gastroenterol Res Pract* 2017; **2017**: 8303046 [PMID: 28947900 DOI: 10.1155/2017/8303046]
 - 9 **Wagner A**, Zandanell S, Kiesslich T, Neureiter D, Klieser E, Holzinger J, Berr F. Systematic Review on Optical Diagnosis of Early Gastrointestinal Neoplasia. *J Clin Med* 2021; **10** [PMID: 34202001 DOI: 10.3390/jcm10132794]
 - 10 **Esteva A**, Kuprel B, Novoa RA, Ko J, Swetter SM, Blau HM, Thrun S. Dermatologist-level classification of skin cancer with deep neural networks. *Nature* 2017; **542**: 115-118 [PMID: 28117445 DOI: 10.1038/nature21056]
 - 11 **Ehteshami Bejnordi B**, Veta M, Johannes van Diest P, van Ginneken B, Karssemeijer N, Litjens G, van der Laak JAWM; the CAMELYON16 Consortium, Hermesen M, Manson QF, Balkenhol M, Geessink O, Stathonikos N, van Dijk MC, Bult P, Beca F, Beck AH, Wang D, Khosla A, Gargeya R, Irshad H, Zhong A, Dou Q, Li Q, Chen H, Lin HJ, Heng PA, Haß C, Bruni E, Wong Q, Halici U, Öner MÜ, Cetin-Atalay R, Berseth M, Khvatkov V, Vylegzhanin A, Kraus O, Shaban M, Rajpoot N, Awan R, Sirinukunwattana K, Qaiser T, Tsang YW, Tellez D, Annuschein J, Hufnagl P, Valkonen M, Kartasalo K, Latonen L, Ruusuvoori P, Liimatainen K, Albarqouni S, Mungal B, George A, Demirci S, Navab N, Watanabe S, Seno S, Takenaka Y, Matsuda H, Ahmady Phoulady H, Kovalev V, Kalinovsky A, Liauchuk V, Bueno G, Fernandez-Carrobles MM, Serrano I, Deniz O, Racoceanu D, Venâncio R. Diagnostic Assessment of Deep Learning Algorithms for Detection of Lymph Node Metastases in Women With Breast Cancer. *JAMA* 2017; **318**: 2199-2210 [PMID: 29234806 DOI: 10.1001/jama.2017.14585]
 - 12 **Bi WL**, Hosny A, Schabath MB, Giger ML, Birkbak NJ, Mehrtash A, Allison T, Arnaout O, Abbosh C, Dunn IF, Mak RH, Tamimi RM, Tempny CM, Swanton C, Hoffmann U, Schwartz LH, Gillies RJ, Huang RY, Aerts HJWL. Artificial intelligence in cancer imaging: Clinical challenges and applications. *CA Cancer J Clin* 2019; **69**: 127-157 [PMID: 30720861 DOI: 10.3322/caac.21552]
 - 13 **Szegedy C**, Liu W, Jia Y, Sermanet P, Reed SE, Anguelov D, Erhan D, Vanhoucke V, Rabinovich A. Going deeper with convolutions. In Proceedings of the IEEE Conference on Computer Vision and Pattern Recognition 2015; 1-x9
 - 14 **Hirasawa T**, Aoyama K, Tanimoto T, Ishihara S, Shichijo S, Ozawa T, Ohnishi T, Fujishiro M, Matsuo K, Fujisaki J, Tada T. Application of artificial intelligence using a convolutional neural network for detecting gastric cancer in endoscopic images. *Gastric Cancer* 2018; **21**: 653-660 [PMID: 29335825 DOI: 10.1007/s10120-018-0793-2]
 - 15 **Van Cutsem E**, Sagaert X, Topal B, Haustermans K, Prenen H. Gastric cancer. *Lancet* 2016; **388**: 2654-2664 [PMID: 27156933 DOI: 10.1016/S0140-6736(16)30354-3]
 - 16 **Karimi P**, Islami F, Anandasabapathy S, Freedman ND, Kamangar F. Gastric cancer: descriptive epidemiology, risk factors, screening, and prevention. *Cancer Epidemiol Biomarkers Prev* 2014; **23**: 700-713 [PMID: 24618998 DOI: 10.1158/1055-9965.EPI-13-1057]
 - 17 **Kono Y**, Kanzaki H, Iwamuro M, Kawano S, Kawahara Y, Okada H. Reality of Gastric Cancer in Young Patients: The Importance and Difficulty of the Early Diagnosis, Prevention and Treatment. *Acta Med Okayama* 2020; **74**: 461-466 [PMID: 33361865 DOI: 10.18926/AMO/61204]
 - 18 **Draganov PV**, Wang AY, Othman MO, Fukami N. AGA Institute Clinical Practice Update: Endoscopic Submucosal Dissection in the United States. *Clin Gastroenterol Hepatol* 2019; **17**: 16-25.e1 [PMID: 30077787 DOI: 10.1016/j.cgh.2018.07.041]
 - 19 **Ono H**, Yao K, Fujishiro M, Oda I, Uedo N, Nimura S, Yahagi N, Iishi H, Oka M, Ajioka Y, Fujimoto K. Guidelines for endoscopic submucosal dissection and endoscopic mucosal resection for early gastric cancer (second edition). *Dig Endosc* 2021; **33**: 4-20 [PMID: 33107115 DOI: 10.1111/den.13883]
 - 20 **Yamazato T**, Oyama T, Yoshida T, Baba Y, Yamanouchi K, Ishii Y, Inoue F, Toda S, Mannen K, Shimoda R, Iwakiri R, Fujimoto K. Two years' intensive training in endoscopic diagnosis facilitates detection of early gastric cancer. *Intern Med* 2012; **51**: 1461-1465 [PMID: 22728475 DOI: 10.2169/internalmedicine.51.7414]
 - 21 **Barbour JA**, O'Toole P, Suzuki N, Dolwani S. Learning endoscopic submucosal dissection in the UK: Barriers, solutions and pathways for training. *Frontline Gastroenterol* 2021; **12**: 671-676 [PMID: 34917325 DOI: 10.1136/flgastro-2020-101526]
 - 22 **Menon S**, Trudgill N. How commonly is upper gastrointestinal cancer missed at endoscopy? *Endosc Int Open* 2014; **2**: E46-E50 [PMID: 26135259 DOI: 10.1055/s-0034-1365524]
 - 23 **Hosokawa O**, Hattori M, Douden K, Hayashi H, Ohta K, Kaizaki Y. Difference in accuracy between gastroscopy and colonoscopy for detection of cancer. *Hepatogastroenterology* 2007; **54**: 442-444 [PMID: 17523293]
 - 24 **Raftopoulos SC**, Segarajasingam DS, Burke V, Ee HC, Yusoff IF. A cohort study of missed and new cancers after esophagogastroduodenoscopy. *Am J Gastroenterol* 2010; **105**: 1292-1297 [PMID: 20068557 DOI: 10.1038/ajg.2009.736]
 - 25 **Yoshimizu S**, Hirasawa T, Horiuchi Y, Omae M, Ishiyama A, Yoshio T, Tsuchida T, Fujisaki J. Differences in upper

- gastrointestinal neoplasm detection rates based on inspection time and esophagogastroduodenoscopy training. *Endosc Int Open* 2018; **6**: E1190-E1197 [PMID: 30302376 DOI: 10.1055/a-0655-7382]
- 26 **Yao K**, Uedo N, Kamada T, Hirasawa T, Nagahama T, Yoshinaga S, Oka M, Inoue K, Mabe K, Yao T, Yoshida M, Miyashiro I, Fujimoto K, Tajiri H. Guidelines for endoscopic diagnosis of early gastric cancer. *Dig Endosc* 2020; **32**: 663-698 [PMID: 32275342 DOI: 10.1111/den.13684]
- 27 **Correa P**, Piazzuelo MB. The gastric precancerous cascade. *J Dig Dis* 2012; **13**: 2-9 [PMID: 22188910 DOI: 10.1111/j.1751-2980.2011.00550.x]
- 28 **Kodama M**, Murakami K, Okimoto T, Abe H, Sato R, Ogawa R, Mizukami K, Shiota S, Nakagawa Y, Soma W, Arita T, Fujioka T. Histological characteristics of gastric mucosa prior to Helicobacter pylori eradication may predict gastric cancer. *Scand J Gastroenterol* 2013; **48**: 1249-1256 [PMID: 24079881 DOI: 10.3109/00365521.2013.838994]
- 29 **Lee KJ**, Inoue M, Otani T, Iwasaki M, Sasazuki S, Tsugane S; JPHC Study Group. Gastric cancer screening and subsequent risk of gastric cancer: a large-scale population-based cohort study, with a 13-year follow-up in Japan. *Int J Cancer* 2006; **118**: 2315-2321 [PMID: 16331632 DOI: 10.1002/ijc.21664]
- 30 **Park SY**, Jeon SW, Jung MK, Cho CM, Tak WY, Kweon YO, Kim SK, Choi YH. Long-term follow-up study of gastric intraepithelial neoplasias: progression from low-grade dysplasia to invasive carcinoma. *Eur J Gastroenterol Hepatol* 2008; **20**: 966-970 [PMID: 18787462 DOI: 10.1097/MEG.0b013e3283013d58]
- 31 **de Vries AC**, van Grieken NC, Looman CW, Casparie MK, de Vries E, Meijer GA, Kuipers EJ. Gastric cancer risk in patients with premalignant gastric lesions: a nationwide cohort study in the Netherlands. *Gastroenterology* 2008; **134**: 945-952 [PMID: 18395075 DOI: 10.1053/j.gastro.2008.01.071]
- 32 **Ezoe Y**, Muto M, Uedo N, Doyama H, Yao K, Oda I, Kaneko K, Kawahara Y, Yokoi C, Sugiura Y, Ishikawa H, Takeuchi Y, Kaneko Y, Saito Y. Magnifying narrowband imaging is more accurate than conventional white-light imaging in diagnosis of gastric mucosal cancer. *Gastroenterology* 2011; **141**: 2017-2025.e3 [PMID: 21856268 DOI: 10.1053/j.gastro.2011.08.007]
- 33 **Zhou F**, Wu L, Huang M, Jin Q, Qin Y, Chen J. The accuracy of magnifying narrow band imaging (ME-NBI) in distinguishing between cancerous and noncancerous gastric lesions: A meta-analysis. *Medicine (Baltimore)* 2018; **97**: e9780 [PMID: 29489678 DOI: 10.1097/MD.0000000000009780]
- 34 **Dohi O**, Yagi N, Yoshida S, Ono S, Sanomura Y, Tanaka S, Naito Y, Kato M. Magnifying Blue Laser Imaging vs Magnifying Narrow-Band Imaging for the Diagnosis of Early Gastric Cancer: A Prospective, Multicenter, Comparative Study. *Digestion* 2017; **96**: 127-134 [PMID: 28848169 DOI: 10.1159/000479553]
- 35 **Fujiyoshi MRA**, Inoue H, Fujiyoshi Y, Nishikawa Y, Toshimori A, Shimamura Y, Tanabe M, Ikeda H, Onimaru M. Endoscopic Classifications of Early Gastric Cancer: A Literature Review. *Cancers (Basel)* 2021; **14** [PMID: 35008263 DOI: 10.3390/cancers14010100]
- 36 **Yu H**, Yang AM, Lu XH, Zhou WX, Yao F, Fei GJ, Guo T, Yao LQ, He LP, Wang BM. Magnifying narrow-band imaging endoscopy is superior in diagnosis of early gastric cancer. *World J Gastroenterol* 2015; **21**: 9156-9162 [PMID: 26290643 DOI: 10.3748/wjg.v21.i30.9156]
- 37 **Yao K**. Clinical Application of Magnifying Endoscopy with Narrow-Band Imaging in the Stomach. *Clin Endosc* 2015; **48**: 481-490 [PMID: 26668793 DOI: 10.5946/ce.2015.48.6.481]
- 38 **Ang TL**, Fock KM, Teo EK, Tan J, Poh CH, Ong J, Ang D. The diagnostic utility of narrow band imaging magnifying endoscopy in clinical practice in a population with intermediate gastric cancer risk. *Eur J Gastroenterol Hepatol* 2012; **24**: 362-367 [PMID: 22198222 DOI: 10.1097/MEG.0b013e3283500968]
- 39 **Ang TL**, Pittayanon R, Lau JY, Rerknimitr R, Ho SH, Singh R, Kwek AB, Ang DS, Chiu PW, Luk S, Goh KL, Ong JP, Tan JY, Teo EK, Fock KM. A multicenter randomized comparison between high-definition white light endoscopy and narrow band imaging for detection of gastric lesions. *Eur J Gastroenterol Hepatol* 2015; **27**: 1473-1478 [PMID: 26426836 DOI: 10.1097/MEG.0000000000000478]
- 40 **Yao K**, Uedo N, Muto M, Ishikawa H, Cardona HJ, Filho ECC, Pittayanon R, Olano C, Yao F, Parra-Blanco A, Ho SH, Avendano AG, Piscocoy A, Fedorov E, Bialek AP, Mitrovic A, Caro L, Gonen C, Dolwani S, Farca A, Cuaresma LF, Bonilla JJ, Kassetsermwiriyaya W, Raganath K, Kim SE, Marini M, Li H, Cimmino DG, Piskorz MM, Iacopini F, So JB, Yamazaki K, Kim GH, Ang TL, Milhomem-Cardoso DM, Waldbaum CA, Carvajal WAP, Hayward CM, Singh R, Banerjee R, Anagnostopoulos GK, Takahashi Y. Development of an E-learning System for the Endoscopic Diagnosis of Early Gastric Cancer: An International Multicenter Randomized Controlled Trial. *EBioMedicine* 2016; **9**: 140-147 [PMID: 27333048 DOI: 10.1016/j.ebiom.2016.05.016]
- 41 **Shibagaki K**, Ishimura N, Yuki T, Taniguchi H, Aimi M, Kobayashi K, Kotani S, Yazaki T, Yamashita N, Tamagawa Y, Mishiro T, Ishihara S, Yasuda A, Kinshita Y. Magnification endoscopy in combination with acetic acid enhancement and narrow-band imaging for the accurate diagnosis of colonic neoplasms. *Endosc Int Open* 2020; **8**: E488-E497 [PMID: 32258370 DOI: 10.1055/a-1068-2056]
- 42 **Russel S**, Norvig P. Artificial Intelligence: A Modern Approach. 2th ed. Pearson Education, 2003
- 43 **Litjens G**, Kooi T, Bejnordi BE, Setio AAA, Ciompi F, Ghafoorian M, van der Laak JAWM, van Ginneken B, Sánchez CI. A survey on deep learning in medical image analysis. *Med Image Anal* 2017; **42**: 60-88 [PMID: 28778026 DOI: 10.1016/j.media.2017.07.005]
- 44 **Yeung S**, Downing NL, Fei-Fei L, Milstein A. Bedside Computer Vision - Moving Artificial Intelligence from Driver Assistance to Patient Safety. *N Engl J Med* 2018; **378**: 1271-1273 [PMID: 29617592 DOI: 10.1056/NEJMp1716891]
- 45 **Nagao S**, Tsuji Y, Sakaguchi Y, Takahashi Y, Minatsuki C, Niimi K, Yamashita H, Yamamichi N, Seto Y, Tada T, Koike K. Highly accurate artificial intelligence systems to predict the invasion depth of gastric cancer: efficacy of conventional white-light imaging, nonmagnifying narrow-band imaging, and indigo-carmin dye contrast imaging. *Gastrointest Endosc* 2020; **92**: 866-873.e1 [PMID: 32592776 DOI: 10.1016/j.gie.2020.06.047]
- 46 **Ikenoyama Y**, Hirasawa T, Ishioka M, Namikawa K, Yoshimizu S, Horiuchi Y, Ishiyama A, Yoshio T, Tsuchida T, Takeuchi Y, Shichijo S, Katayama N, Fujisaki J, Tada T. Detecting early gastric cancer: Comparison between the diagnostic ability of convolutional neural networks and endoscopists. *Dig Endosc* 2021; **33**: 141-150 [PMID: 32282110 DOI: 10.1111/den.13688]

- 47 **Nam JY**, Chung HJ, Choi KS, Lee H, Kim TJ, Soh H, Kang EA, Cho SJ, Ye JC, Im JP, Kim SG, Kim JS, Chung H, Lee JH. Deep learning model for diagnosing gastric mucosal lesions using endoscopic images: development, validation, and method comparison. *Gastrointest Endosc* 2022; **95**: 258-268.e10 [PMID: 34492271 DOI: 10.1016/j.gie.2021.08.022]
- 48 **Ling T**, Wu L, Fu Y, Xu Q, An P, Zhang J, Hu S, Chen Y, He X, Wang J, Chen X, Zhou J, Xu Y, Zou X, Yu H. A deep learning-based system for identifying differentiation status and delineating the margins of early gastric cancer in magnifying narrow-band imaging endoscopy. *Endoscopy* 2021; **53**: 469-477 [PMID: 32725617 DOI: 10.1055/a-1229-0920]
- 49 **Wu L**, Wang J, He X, Zhu Y, Jiang X, Chen Y, Wang Y, Huang L, Shang R, Dong Z, Chen B, Tao X, Wu Q, Yu H. Deep learning system compared with expert endoscopists in predicting early gastric cancer and its invasion depth and differentiation status (with videos). *Gastrointest Endosc* 2022; **95**: 92-104.e3 [PMID: 34245752 DOI: 10.1016/j.gie.2021.06.033]
- 50 **Cho BJ**, Bang CS, Park SW, Yang YJ, Seo SI, Lim H, Shin WG, Hong JT, Yoo YT, Hong SH, Choi JH, Lee JJ, Baik GH. Automated classification of gastric neoplasms in endoscopic images using a convolutional neural network. *Endoscopy* 2019; **51**: 1121-1129 [PMID: 31443108 DOI: 10.1055/a-0981-6133]
- 51 **Wu L**, Xu M, Jiang X, He X, Zhang H, Ai Y, Tong Q, Lv P, Lu B, Guo M, Huang M, Ye L, Shen L, Yu H. Real-time artificial intelligence for detecting focal lesions and diagnosing neoplasms of the stomach by white-light endoscopy (with videos). *Gastrointest Endosc* 2022; **95**: 269-280.e6 [PMID: 34547254 DOI: 10.1016/j.gie.2021.09.017]
- 52 **Wu L**, He X, Liu M, Xie H, An P, Zhang J, Zhang H, Ai Y, Tong Q, Guo M, Huang M, Ge C, Yang Z, Yuan J, Liu J, Zhou W, Jiang X, Huang X, Mu G, Wan X, Li Y, Wang H, Wang Y, Chen D, Gong D, Wang J, Huang L, Li J, Yao L, Zhu Y, Yu H. Evaluation of the effects of an artificial intelligence system on endoscopy quality and preliminary testing of its performance in detecting early gastric cancer: a randomized controlled trial. *Endoscopy* 2021; **53**: 1199-1207 [PMID: 33429441 DOI: 10.1055/a-1350-5583]
- 53 **Kubota K**, Kuroda J, Yoshida M, Ohta K, Kitajima M. Medical image analysis: computer-aided diagnosis of gastric cancer invasion on endoscopic images. *Surg Endosc* 2012; **26**: 1485-1489 [PMID: 22083334 DOI: 10.1007/s00464-011-2036-z]
- 54 **Zhu Y**, Wang QC, Xu MD, Zhang Z, Cheng J, Zhong YS, Zhang YQ, Chen WF, Yao LQ, Zhou PH, Li QL. Application of convolutional neural network in the diagnosis of the invasion depth of gastric cancer based on conventional endoscopy. *Gastrointest Endosc* 2019; **89**: 806-815.e1 [PMID: 30452913 DOI: 10.1016/j.gie.2018.11.011]
- 55 **Ishioka M**, Hirasawa T, Tada T. Detecting gastric cancer from video images using convolutional neural networks. *Dig Endosc* 2019; **31**: e34-e35 [PMID: 30449050 DOI: 10.1111/den.13306]
- 56 **Yoon HJ**, Kim S, Kim JH, Keum JS, Oh SI, Jo J, Chun J, Youn YH, Park H, Kwon IG, Choi SH, Noh SH. A Lesion-Based Convolutional Neural Network Improves Endoscopic Detection and Depth Prediction of Early Gastric Cancer. *J Clin Med* 2019; **8** [PMID: 31454949 DOI: 10.3390/jcm8091310]
- 57 **Tang D**, Wang L, Ling T, Lv Y, Ni M, Zhan Q, Fu Y, Zhuang D, Guo H, Dou X, Zhang W, Xu G, Zou X. Development and validation of a real-time artificial intelligence-assisted system for detecting early gastric cancer: A multicentre retrospective diagnostic study. *EBioMedicine* 2020; **62**: 103146 [PMID: 33254026 DOI: 10.1016/j.ebiom.2020.103146]
- 58 **Namikawa K**, Hirasawa T, Nakano K, Ikenoyama Y, Ishioka M, Shiroma S, Tokai Y, Yoshimizu S, Horiuchi Y, Ishiyama A, Yoshio T, Tsuchida T, Fujisaki J, Tada T. Artificial intelligence-based diagnostic system classifying gastric cancers and ulcers: comparison between the original and newly developed systems. *Endoscopy* 2020; **52**: 1077-1083 [PMID: 32503056 DOI: 10.1055/a-1194-8771]
- 59 **Ueyama H**, Kato Y, Akazawa Y, Yatagai N, Komori H, Takeda T, Matsumoto K, Ueda K, Hojo M, Yao T, Nagahara A, Tada T. Application of artificial intelligence using a convolutional neural network for diagnosis of early gastric cancer based on magnifying endoscopy with narrow-band imaging. *J Gastroenterol Hepatol* 2021; **36**: 482-489 [PMID: 32681536 DOI: 10.1111/jgh.15190]
- 60 **Oura H**, Matsumura T, Fujie M, Ishikawa T, Nagashima A, Shiratori W, Tokunaga M, Kaneko T, Imai Y, Oike T, Yokoyama Y, Akizue N, Ota Y, Okimoto K, Arai M, Nakagawa Y, Inada M, Yamaguchi K, Kato J, Kato N. Development and evaluation of a double-check support system using artificial intelligence in endoscopic screening for gastric cancer. *Gastric Cancer* 2022; **25**: 392-400 [PMID: 34652556 DOI: 10.1007/s10120-021-01256-8]
- 61 **Zhang L**, Zhang Y, Wang L, Wang J, Liu Y. Diagnosis of gastric lesions through a deep convolutional neural network. *Dig Endosc* 2021; **33**: 788-796 [PMID: 32961597 DOI: 10.1111/den.13844]
- 62 **An P**, Yang D, Wang J, Wu L, Zhou J, Zeng Z, Huang X, Xie Y, Hu S, Chen Y, Yao F, Guo M, Wu Q, Yang Y, Yu H. A deep learning method for delineating early gastric cancer resection margin under chromoendoscopy and white light endoscopy. *Gastric Cancer* 2020; **23**: 884-892 [PMID: 32356118 DOI: 10.1007/s10120-020-01071-7]
- 63 **Miyaki R**, Yoshida S, Tanaka S, Kominami Y, Sanomura Y, Matsuo T, Oka S, Raytchev B, Tamaki T, Koide T, Kaneda K, Yoshihara M, Chayama K. Quantitative identification of mucosal gastric cancer under magnifying endoscopy with flexible spectral imaging color enhancement. *J Gastroenterol Hepatol* 2013; **28**: 841-847 [PMID: 23424994 DOI: 10.1111/jgh.12149]
- 64 **Miyaki R**, Yoshida S, Tanaka S, Kominami Y, Sanomura Y, Matsuo T, Oka S, Raytchev B, Tamaki T, Koide T, Kaneda K, Yoshihara M, Chayama K. A computer system to be used with laser-based endoscopy for quantitative diagnosis of early gastric cancer. *J Clin Gastroenterol* 2015; **49**: 108-115 [PMID: 24583752 DOI: 10.1097/MCG.000000000000104]
- 65 **Kanesaka T**, Lee TC, Uedo N, Lin KP, Chen HZ, Lee JY, Wang HP, Chang HT. Computer-aided diagnosis for identifying and delineating early gastric cancers in magnifying narrow-band imaging. *Gastrointest Endosc* 2018; **87**: 1339-1344 [PMID: 29225083 DOI: 10.1016/j.gie.2017.11.029]
- 66 **Li L**, Chen Y, Shen Z, Zhang X, Sang J, Ding Y, Yang X, Li J, Chen M, Jin C, Chen C, Yu C. Convolutional neural network for the diagnosis of early gastric cancer based on magnifying narrow band imaging. *Gastric Cancer* 2020; **23**: 126-132 [PMID: 31332619 DOI: 10.1007/s10120-019-00992-2]
- 67 **Horiuchi Y**, Aoyama K, Tokai Y, Hirasawa T, Yoshimizu S, Ishiyama A, Yoshio T, Tsuchida T, Fujisaki J, Tada T. Convolutional Neural Network for Differentiating Gastric Cancer from Gastritis Using Magnified Endoscopy with Narrow Band Imaging. *Dig Dis Sci* 2020; **65**: 1355-1363 [PMID: 31584138 DOI: 10.1007/s10620-019-05862-6]
- 68 **Hu H**, Gong L, Dong D, Zhu L, Wang M, He J, Shu L, Cai Y, Cai S, Su W, Zhong Y, Li C, Zhu Y, Fang M, Zhong L, Yang X, Zhou P, Tian J. Identifying early gastric cancer under magnifying narrow-band images with deep learning: a

- multicenter study. *Gastrointest Endosc* 2021; **93**: 1333-1341.e3 [PMID: 33248070 DOI: 10.1016/j.gie.2020.11.014]
- 69 **Hamada K**, Kawahara Y, Tanimoto T, Ohto A, Toda A, Aida T, Yamasaki Y, Gotoda T, Ogawa T, Abe M, Okanoue S, Takei K, Kikuchi S, Kuroda S, Fujiwara T, Okada H. Application of convolutional neural networks for evaluating the depth of invasion of early gastric cancer based on endoscopic images. *J Gastroenterol Hepatol* 2022; **37**: 352-357 [PMID: 34713495 DOI: 10.1111/jgh.15725]
- 70 **Panarese A**, Galatola G, Armentano R, Pimentel-Nunes P, Ierardi E, Caruso ML, Pesce F, Lenti MV, Palmitessa V, Coletta S, Shahini E. *Helicobacter pylori*-induced inflammation masks the underlying presence of low-grade dysplasia on gastric lesions. *World J Gastroenterol* 2020; **26**: 3834-3850 [PMID: 32774061 DOI: 10.3748/wjg.v26.i26.3834]
- 71 **Shichijo S**, Nomura S, Aoyama K, Nishikawa Y, Miura M, Shinagawa T, Takiyama H, Tanimoto T, Ishihara S, Matsuo K, Tada T. Application of Convolutional Neural Networks in the Diagnosis of *Helicobacter pylori* Infection Based on Endoscopic Images. *EBioMedicine* 2017; **25**: 106-111 [PMID: 29056541 DOI: 10.1016/j.ebiom.2017.10.014]
- 72 **Itoh T**, Kawahira H, Nakashima H, Yata N. Deep learning analyzes *Helicobacter pylori* infection by upper gastrointestinal endoscopy images. *Endosc Int Open* 2018; **6**: E139-E144 [PMID: 29399610 DOI: 10.1055/s-0043-120830]



Basic Study

Learning models for colorectal cancer signature reconstruction and classification in patients with chronic inflammatory bowel disease

Mariem Abaach, Ian Morilla

Specialty type: Mathematical and computational biology

Provenance and peer review: Invited article; Externally peer reviewed.

Peer-review model: Single blind

Peer-review report's scientific quality classification

Grade A (Excellent): A

Grade B (Very good): B

Grade C (Good): 0

Grade D (Fair): 0

Grade E (Poor): 0

P-Reviewer: Bertani L, Italy; Sasaki LY, Brazil

Received: December 9, 2021

Peer-review started: December 9, 2021

First decision: January 26, 2022

Revised: February 16, 2022

Accepted: April 28, 2022

Article in press: April 28, 2022

Published online: April 28, 2022



Mariem Abaach, Mathématiques Appliquées à Paris 5, Unité mixte de Recherche, Centre National de la Recherche Scientifique, Université de Paris, Paris 75006, France

Ian Morilla, Laboratoire Analyse, Géométrie et Applications, Centre National de la Recherche Scientifique (Unité mixte de Recherche), Université Sorbonne Paris Nord, Villetaneuse, Paris 93430, France

Corresponding author: Ian Morilla, PhD, Assistant Professor, Research Associate, Laboratoire Analyse, Géométrie et Applications, Centre National de la Recherche Scientifique (Unité mixte de Recherche), Université Sorbonne Paris Nord, 99 avenue Jean Baptiste clément, Villetaneuse, Paris 93430, France. morilla@math.univ-paris13.fr

Abstract

BACKGROUND

In their everyday life, clinicians face an overabundance of biological indicators potentially helpful during a disease therapy. In this context, to be able to reliably identify a reduced number of those markers showing the ability of optimising the classification of treatment outcomes becomes a factor of vital importance to medical prognosis. In this work, we focus our interest in inflammatory bowel disease (IBD), a long-life threaten with a continuous increasing prevalence worldwide. In particular, IBD can be described as a set of autoimmune conditions affecting the gastrointestinal tract whose two main types are Crohn's disease and ulcerative colitis.

AIM

To identify the minimal signature of microRNA (miRNA) associated with colorectal cancer (CRC) in patients with one chronic IBD.

METHODS

We provide a framework of well-established statistical and computational learning methods wisely adapted to reconstructing a CRC network leveraged to stratify these patients.

RESULTS

Our strategy resulted in an adjusted signature of 5 miRNAs out of approximately 2600 in Crohn's Disease (resp. 8 in Ulcerative Colitis) with a percentage of success in patient classification of 82% (resp. 81%).

CONCLUSION

Importantly, these two signatures optimally balance the proportion between the number of significant miRNAs and their percentage of success in patients' stratification.

Key Words: Inflammatory bowel disease; microRNA; Multi-group comparison; Machine learning; Colorectal cancer; Sparse partial least squares-discriminant analysis

©The Author(s) 2022. Published by Baishideng Publishing Group Inc. All rights reserved.

Core Tip: This study provides an optimised strategy based on classic learning methods and multi-group variable selection combination from 2600 microRNAs of 225 patients with one chronic inflammatory bowel disease to identify the minimal signature of microRNAs associated with the development of colorectal cancer in these patients.

Citation: Abaach M, Morilla I. Learning models for colorectal cancer signature reconstruction and classification in patients with chronic inflammatory bowel disease. *Artif Intell Cancer* 2022; 3(2): 27-41

URL: <https://www.wjgnet.com/2644-3228/full/v3/i2/27.htm>

DOI: <https://dx.doi.org/10.35713/aic.v3.i2.27>

INTRODUCTION

The emergence of high-through experiments, image-based analysis and massive sequencing techniques [1-3] has disrupted the way clinicians make decision on a disease therapy. Now the usage of the grade of expertise in their respective domains to decide a treatment, frequently considered as a subjective evaluation, is strengthened by an overwhelming capability of support. However, this overabundance of available information does not make their task that straightforward. In this context, the use of interpretable mathematical methods can decipher the underlying complexity of data, generating systemic hypothesis that really help practitioners with their treatment outcomes. In this study, we introduce a learning framework based on a combination between unsupervised hierarchical clustering and weakly supervised classification approaches. These methods are applied to the analysis of a pool with approximately 6000 miRNAs extracted from biopsies of 216 inflammatory bowel disease (IBD) patients with and without colorectal cancer (CRC).

IBD consist of various disorders that cause prolonged inflammation of the digestive tract. Its prevalence rises more and more in the western developed countries[4] largely affecting their health-care systems. Besides that fact, the treatment of such disorders requires an early assessment of the response to the medical treatment[5]. Thus, the finding of a reduced signature optimally predicting the strata a patient will be lying on is of paramount importance during therapy. The main goal of our methodology is using the above approaches to reconstructing a minimal network that stratifies patients with a chronic IBD[5,6] having developed CRC as indicated in[7,8].

Unsupervised hierarchical clustering[5] is a robust method successfully used in the comparison of more than two groups. Particularly, this method enables the identification of biologically meaningful biomarkers, *i.e.* miRNAs, reducing significantly the amount of data in the study. Powered by sparse partial least squares discriminant analysis (sPLS-DA) this signature becomes minimal[9] in the description of the required CRC network in IBD. And the later application of random forests (RF)[10] and support vector machines (SVM)[11,12] to the adjusted signature of selected miRNAs ensures the classification of patients is less sensitive to data heterogeneity. Regarding the calibration of classifiers, the performance of each algorithm is assessed by means of leave-one-out (LOO) cross validation[13] and their confusion matrices[14]. Overall this methodology shortens clinicians' efforts, enhancing a reduced set of important features and avoiding unnecessary time delays prior to make any decision on the course of a disease therapy.

Motivation

There exist intra patient differences in miRNA expression between the inflammatory and healthy tissue, between the healthy tissue of an inflammatory and non-inflammatory patient and between the healthy tissue of a cancer and non- cancer colic patient. We want to identify a minimal miRNA profile of developing or not cancer in patients with a chronic inflammatory bowel disease. In other words, a miRNA profile of healthy tissue from patients with chronic IBD with (case) *vs* without cancer (control). In that way, provided a specific miRNA profile is of interest, this one could be prospectively validated, and its predictive marker maybe also developed. Ultimately, this would allow clinicians to increase the diagnosis colonoscopy pace in IBD patients where a miRNA profile of risk is detected and conversely

decreasing that pace in patients tagged as at lower risk.

MATERIALS AND METHODS

Samples and mi RNA extractions

Patients were recruited from various public French hospitals for this study. Our sample consists of 225 IBD patients with 75 cases developing dysplasia in colon. These cases matched with 150 controls, *i.e.*, patients with IBD who did not develop dysplasia, yielding a total ratio of 1 case for each 2 controls. The extraction of 6609 miRNAs in each sample resulted from the biopsies of 216 quantified patients. A posteriori, 10 out of these 216 patients were discarded because of their difficulty in extracting miRNAs.

Biological variability

At least 40 biopsies were extracted from each sample during diagnostic chromo-endoscopies in IBD. The anatomopathological grading of inflammation described in [15,16] is adopted on the Hematoxylin Eosin Saffron slide of each sample. To not get affected the miRNA signature by a mucosa inflammation, only the healthy mucosa (non-inflammatory nor dysplastic) corresponding to the grade 0 in GOMES classification was collected. Finally, the absence of histological inflammatory lesion in the mucosa has been considered in preference to the colic segments.

Quality control

Following the Affymetrix hybridisation standards [17], the intensity of miRNA was log₂-transformed (Supplementary Figure 1). A first quality control on all miRNA was performed using a principal component analysis (PCA). PCA by [18] allows transforming a set of correlated data, herein their intensity in the gene-chip of Affymetrix GeneChip miRNA 4.0 chips, in a new data set, uncorrelated, by following the top ranked principal components. These components are used as axes of a new space where detect patients with an ambiguous score of intensity, *i.e.*, those intensity outputs generated by unsuitable experimental condition, and exclude them all. Just after one of the two RNA strands becomes functional the miRNA is prepared to participate in intricate biological processes within the cell. This maturation process leads the miRNA to a “steady-state” that provides a more valuable biological information. Thus, we opted for considering only mature transcript miRNAs defined in [19], noted by MIMAT, in the completion of this study. Those transcripts amount to 2578 miRNAs in total. In addition, miRNAs with an average intensity > 8 were also removed being considered as outliers of the overall expression profile.

Technical variability

The Affymetrix Genechip 4.0 encompasses around 36000 probes, more than 6000 of which are humans (each probe corresponds to a complementary sequence of nucleotides). Details on each miRNA and sample are provided by the Affymetrix database. The intensity values of 6609 miRNAs are considered from the 216 patients. Notably, both the RNA extraction and the miRNA technical analysis were performed twice with similar library sizes (see Supplemental Material) detecting a very low bias attributable to a defective sample collection or a poor miRNA quality.

STATISTICAL LEARNING ANALYSIS

Reconstruction of the miRNA signature

Differential expression using general linear models: A first signature of differentially expressed (DE) miRNAs is inferred from general linear models implemented in the limma R-package [20]. During this process we estimate variance for other miRNAs, weight to incorporate unequal variations in data, and pre-process to reduce noise.

Multiclass DE analysis: The signature identified by linear models returned an amount of miRNAs larger than expected to be considered in practice as biologically significant. We decided, then, to reduce the size of miRNA signature by means of a multi-group comparison strategy. Firstly, we calculated the mean expression of each miRNA according to the four analysed groups [*i.e.*, Ulcerative colitis (UC) and Crohn’s disease (CD) cases and controls respectively]. Next, we construct the tree related groups. Thus, we assume an underlying tree structure to compare groups based on recursive binary splits along the tree. Then each mean expression was compared, using a simple *t* test as in [21]. Any miRNA with a significant *t* test (*i.e.*, threshold = 0.005) was included in the final model.

We propose different strategies to test in pairwise all the possible combinations of groups: (1) Use the CD patients or the UC patients exclusively; and (2) Use each one of the groups to construct the tree (Figure 1 and Table 1): (1) Strategy 1: Comparison between the CD controls and the three remaining leaves (UC controls, CD cases and UC cases), then UC controls compare to CD cases and UC cases, *etc.*;

Table 1 Possible comparisons to be made during the unsupervised (i.e., we do not rely on the type of disease) global analysis of patients following the considered three different strategies

Strategy	Comparison
Strategy 1 (classic)	1 vs (2,3,4)
	2 vs (3,4)
	3 vs 4
Strategy 2 (1&1)	1 vs 2; 1 vs 3; 1 vs 4
	2 vs 1; 2 vs 3; 2 vs 4
	3 vs 1; 3 vs 2; 3 vs 4
	4 vs 1; 4 vs 2; 4 vs 3
Strategy 3 (pairwise)	1 vs (2,3,4)
	2 vs (1,3,4)
	3 vs (1,2,4)
	4 vs (1,2,3)

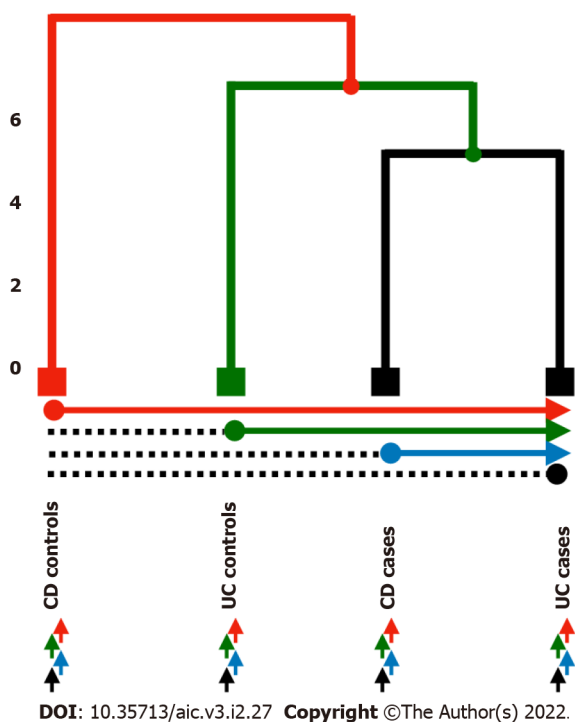


Figure 1 Pairwise leaves comparison to be tested. Hierarchical structure amounts to strategy 1 while horizontal and bottom arrows describe strategies 2 and 3 respectively. Highlighted in red, green, blue, and black the 4 possible comparisons amongst group of patients. UC: Ulcerative colitis; CD: Crohn’s disease.

- (2) Strategy 2: Comparison between each leaf and the others; CD controls compare to UC controls, CD cases and UC cases, then UC controls compare to CD controls and cases, and UC cases, and so on;
- (3) Strategy 3: Comparison among leaves one by one; CD controls compare to UC controls, then CD controls compare to CD cases, and so on.

Upon setting the methodology, we analyse two related data set in tandem. Initially, we applied the method only to the miRNA labeled as MIMAT; to repeat the same approach, on a second occasion, with a set of 152 miRNAs previously selected by sparse PLS Discriminant Analysis (sPLS-DA).

In brief, PLS is an exploratory variable selection technique successfully proven in classification[22]. In particular, the sPLS-DA[9] is an extension of PLS applied in multi-class classification. It selects the most discriminant variables to classify patients, using Lasso penalization. By means of the mixOmics R package[23] three components of miRNAs were identified to predict cancer in all patients. The number of selected variables for each of the three components was chosen based on the lowest average balanced classification error rate with centroids after tuning of the sPLS-DA model using the selected number of

components and 5-fold cross-validation with 10 repeats. The linear programming problem associated with sPLS-DA may be succinctly described as:

Where $\min_{u_i, v_i} \|M_i - u_i v_i^T\|_F^2 + P_\lambda u_i$, is applied component-wise in the vector $P_\lambda(u_i) = \text{sign}(u_i)(|u_i| - \lambda)_+$ (*i.e.*, the left singular vector from the Singular Value Decomposition (SVD) of the miRNA matrix expression M) and acts as the relaxed thresholding function that scales the Lasso penalty functions[24]. Thus, λ is the penalization parameter to tune.

Each sPLS-DA axis is constructed by a convex linear combination of a miRNA. Hence, the coordinate of any given patient on that axis is described by:

$$\sum_{i=1}^N \alpha_i \times \text{miRNA}_i$$

Then applying the majority vote criterion, any given individual having been calculated to have a probability > 0.5 in at least 2 out of 3 PLS-DA axes is considered misclassified.

Classification of patients

In an early exploratory classification, we based our results on the Euclidian distance of miRNA intensities across patients. Nevertheless, the high sensitivity of the Euclidean-based norm to heterogeneous data and non-linearity produced a poor classification (Supplementary Figure 2). Anyway, this first classification definitively clued us in on the miRNA signature's optimisation. Next, to prevent the non-linear effect of our measurements in classification, we contemplated the employment of learning methods. Thus, the main purpose random forests and support vector machines pursue is the reconstruction of a minimal CRC network that could lead to optimally stratify the IBD patients evaluating the associated miRNA signature. These two methods are powerful tools to predict patients developing CRC that perform well in different classification issues. Briefly, RF is a machine learning method for classification based on decision tree and probabilities, introduced in[10], whereas SVM is a strong classifier with the aim of finding the optimal separation hyperplane of data by maximising the margin [25]. A total of 5,000 trees were conducted for RF analysis. The SVM was implemented using a linear

kernel, *i.e.*, $K(x_i, x_j) = \exp\left(\frac{-\|x_i - x_j\|^2}{2\sigma^2}\right)$ with bandwidth and including soft-regularisation with Sequential Minimal Optimization (SMO) as solver to find the optimal hyperplane well separating classes. The general out-put of a binary SVM classifier can be computed by the following expression:

$$y = \text{sign}\left(\sum_{i=1}^N \alpha_i y_i K(x_i, x_j) + b\right)$$

where $\alpha_i \geq 0$ are Lagrangian multipliers obtained by solving a quadratic optimisation problem, b is the bias, and K is the above defined kernel function. We evaluated the performance of each patient's classification using cross-validation with the LOO method. The RF classification was performed using the *randomForest* function of the *random-Forest* R-package[26]. Complementary, the variable importance (VIMP) of each miRNA for RF[27] was also calculated using the *varImp* and *varImpPlot* functions of the same pack- age. The Matlab® classification app implemented the SVM analysis and results are confirmed using *svm* function of the *e1071* R-package.

Performance evaluation of classification methods

We evaluate how optimal a miRNA signature is by means of its confusion matrix, using the *confusion-Matrix* function of the *caret* R-package[28], and the so-called Receiver Operating Characteristic (ROC) curve along the calculus of its area under curve (AUC) using the *plotROC* R-package[29]. Percentage of true classification, sensibility, specificity, and the AUC were also calculated for each strategy using these two packages.

In summary, all the calculations of the statistical learning analysis were implemented using in-house scripts based on R and Matlab® (2014a, The MathWorks Inc., Natick, MA), and figures were depicted with *ggplot2* R-package.

RESULTS

A previous work of denoising is required if we want to reduce possible issues of bias and overfitting in our algorithms. Thus, the analysis was performed on 206 patients; excluding 4 patients considered as outliers, and 6 unmatched controls with cases. In addition, 101 miRNAs were removed since their expression was higher than 8. These miRNAs highly influenced to broke inconsistently down large clusters in the construction of tree and though considered as outliers. Yet, note that the unsupervised clustering can be biased by the lack of linearity in data. Hence, the way we use the hierarchical classification is limited to track a definite signature trend to be further learned by more robust methods. The best result was always obtained by the strategy 1. For clarity, we only show those results yielded by

Table 2 Summary of patients' classification predicted by random forests/support vector machines respectively. From left to right: Group of patients, amount of selected miRNA, percentage of success in true positive classification, sensitivity, specificity and their area under the curve

Methods	N° miRNA	% True classification (95%CI)	Sensitivity	Specificity	AUC
All miRNA					
Strategy 1	56	69 (62-75)/69 (62-75)	0.25/0.43	0.93/0.83	0.76/0.74
CD	9	87 (78-93)/86 (77-92)	0.70/0.73	0.96/0.93	0.89/0.92
UC	30	72% (63-80)/76 (67-83)	0.45/0.55	0.86/0.87	0.77/0.81
miRNAs selected by sPLS-DA					
Strategy 1	11	69 (62-75)/68 (62-75)	0.36/0.36	0.87/0.86	0.72/0.74
CD	5	80 (70-88)/82 (67-86)	0.67/0.60	0.87/0.87	0.84/0.86
UC	8	73 (64-80)/81 (73-88)	0.48/0.57	0.86/0.93	0.73/0.81

AUC: Area under curve; CD: Crohn's disease; UC: Ulcerative colitis.

Table 3 All patients contingency matrix of the 56-selected miRNAs by means of random forests and support vector machines methods

Predicted by RF		Predicted by SVM			
		Cases	Controls	Cases	Controls
True	Case	18	54	31	41
	Controls	10	124	23	111

RF: Random forests; SVM: Support vector machines.

means of this strategy. We address to supplemental material for further details on the other two remaining strategies (Supplementary Figures 3-5 and 7-8). Naturally, the performance of this approach depends on each initial tree re- construction. The Table 2 summaries patients classification performed by all the methods using the strategy 1.

The overall signature associated with CRC

A priori, one would expect to find here a tree with two well separated branches making distinction between CD and UC patients. Nevertheless, the tree this first comparison returned describes a structure composed of three branches that mixes up cases with controls. Hence, the primary leaf groups the CD cases, the second one binds UC cases together, whereas the third leaf consists of control patients. See Supplementary Figure 1 to visualise the tree corresponding to the analysis of all the IBD patients.

Strategy 1: When this first strategy is considered, we are able to identify 56 miRNAs whose expression is differential between the CRC cases and controls. Those miRNAs are potentially good candidates to be associated with a CRC network that can achieve an optimal stratification of patients. A heatmap enhancing these miRNAs are depicted below in Figure 2. However, data heterogeneity and non-linearity negatively influence the measures captured by our multi-class strategy producing a poor stratification performance when re- constructing the sought minimal CRC network. To overcome such an obstacle, we keep using the selected miRNAs, but applied to classifiers such as RF and SVM which are more robust in presence of non-linear heterogeneous data. This combination enables better learning how patients stratify according to CRC. In that way, we attained to correctly classify the 69% of patients by means of RF and using linear SVM (see Table 2 and Figure 2B and C). However, the SVM performance overtakes at large that one given by RF in every case of patient stratification. Notice the large number of selected miRNAs in this first analysis. For clarity, the VIMP analysis shown in Supplementary Figure 6A only discloses the top 30 miRNA. The results obtained in the performance of patients' classification is represented as a confusion matrix in Table 3. In general control patients were correctly classified, but a remarkable number of cases was muddled with controls. This situation can be explained by the, pointed out in the literature, divergent genetic source of the two types of IBD. The ROC curve displayed in Figure 2B and C reported sensitivity-specificity ranges of 0.25-0.93 and 0.43-0.83 associated with RF and SVM respectively (Table 2).

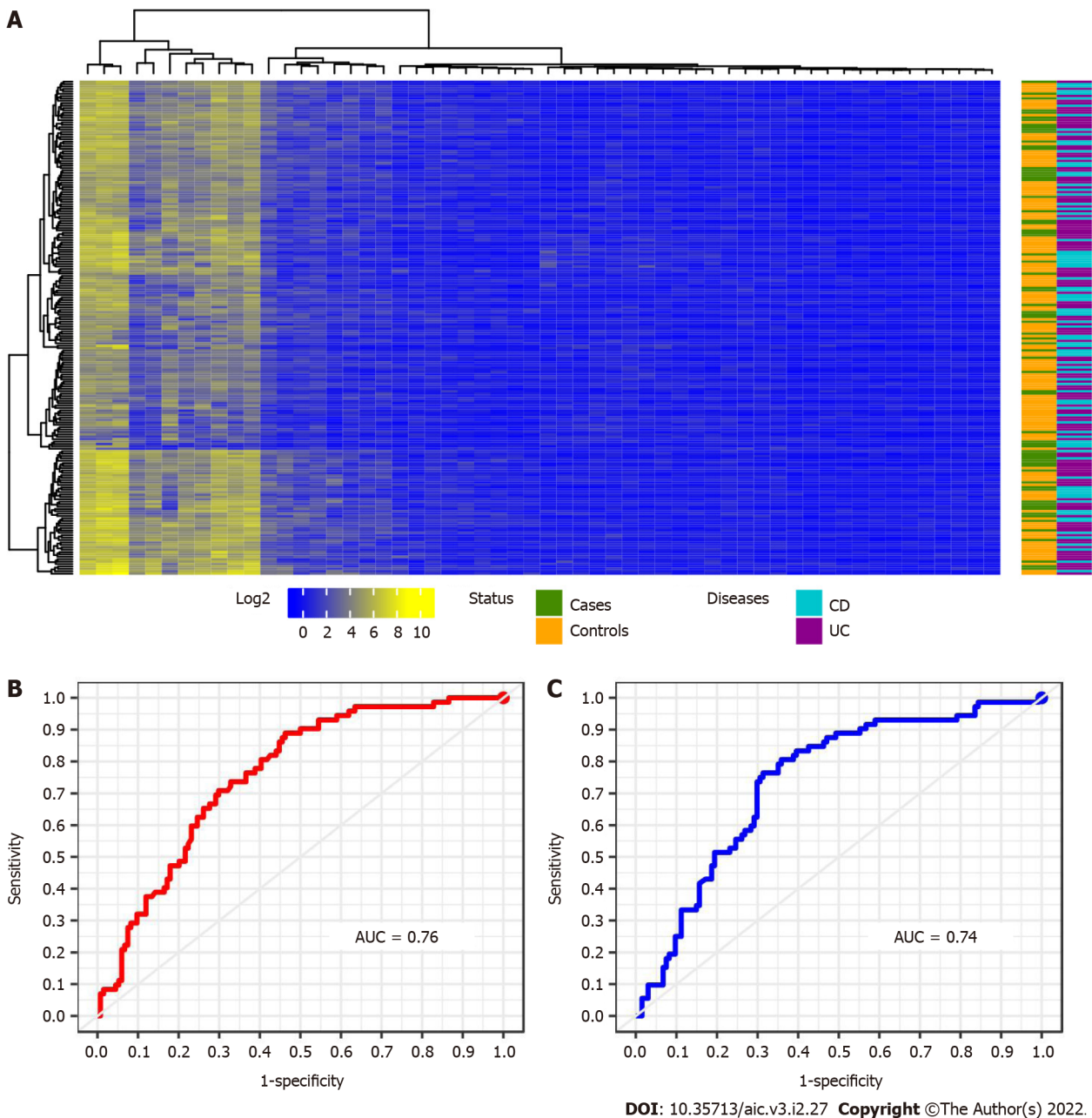


Figure 2 All patients hierarchical and leaning performance. A: Heatmap of the 56- selected miRNA intensity. Colour corresponding to the status of the patients: Purple: Ulcerative colitis patients; light blue: Crohn’s disease patients; green: cases and yellow: Controls; B: Receiver operating characteristic curve for the classification using random forests analysis; C: Using L-SVM models for the 56 selected miRNA. AUC: Area under the curve.

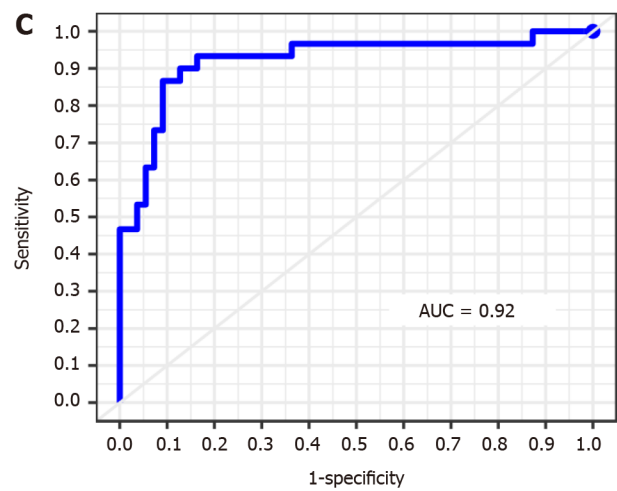
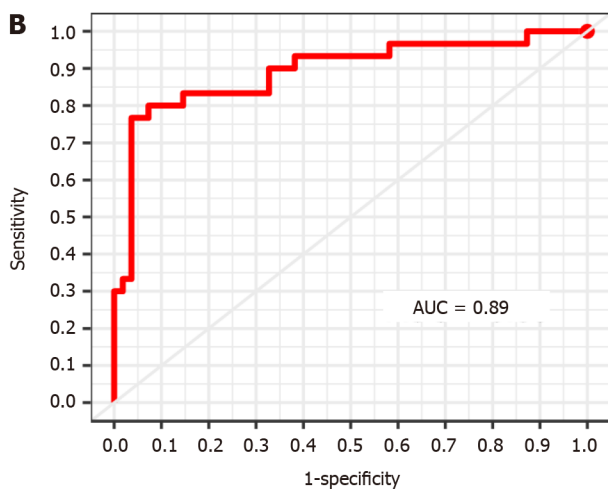
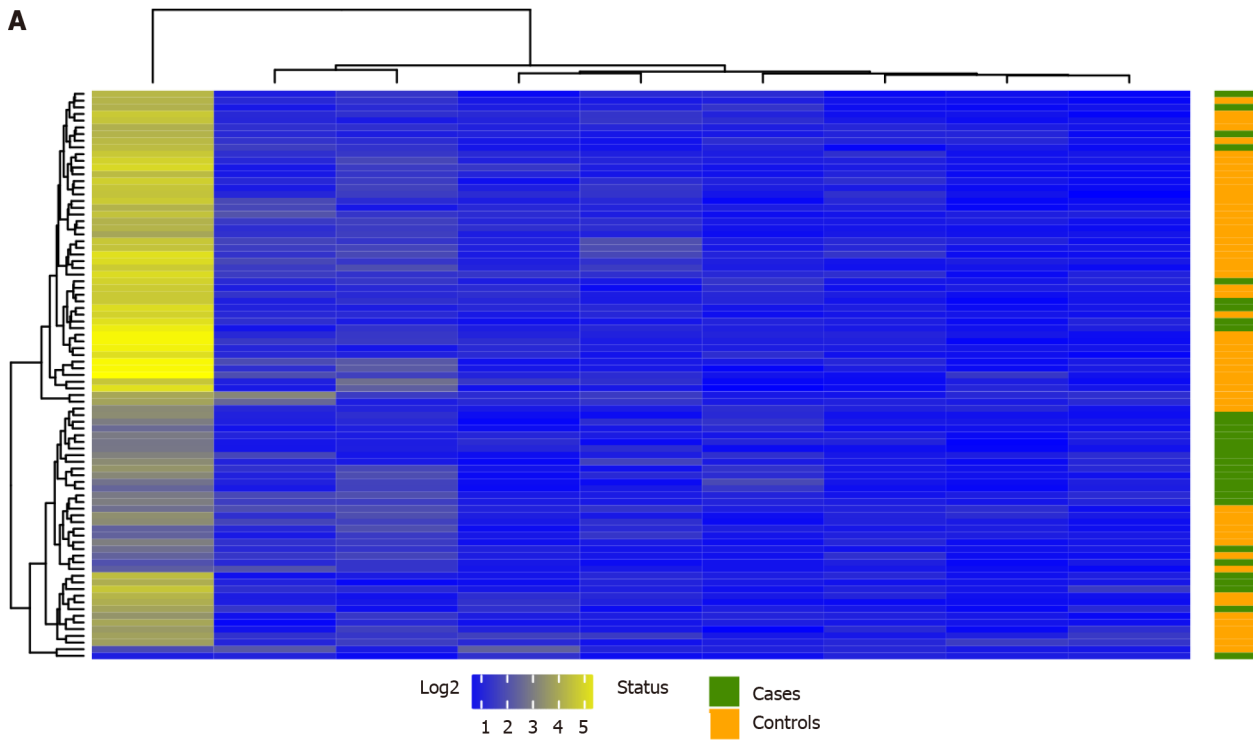
Constructing the local signature of CD patients

For this analysis we provide a sample data composed of 85 patients with CD, whose 30 are cases and 55 controls. As observed in panel (A) of Figure 3, we detect 9 miRNAs differentially expressed between cases and control in CD patients. But the use of the Euclidian distance misleads their percent- age of classification as occurred in the previous case-control study. The results obtained by the above indicated RF and SVM learning methods may be observed in Figure 3B and C and Table 2. The variable importance of each miRNA is also considered to simplify the calibration of the RF models (data not shown, see Supplementary Figure 6B). Moreover, their associated sensitivity-specificity ranges are 0.70-0.73 and 0.96-0.93 to RF and SVM respectively (Table 2). With these selected miRNAs, patients are correctly classified in the 87% and 86% of cases. These percentages are also shown in terms of a confusion matrix in Table 4. The adopted non supervised - supervised strategy returns rather good candidates to conform the network associate to CRC in IBD also providing the signature with an accurate predictive ability.

Table 4 Contingence matrix of the 9-selected miRNA and random forests methods for Crohn's disease patients

Predicted by RF		Predicted by SVM			
		Cases	Controls	Cases	Controls
True	Case	21	9	22	4
	Controls	2	53	8	51

RF: Random forests; SVM: Support vector machines.



DOI: 10.35713/aic.v3.i2.27 Copyright ©The Author(s) 2022.

Figure 3 Crohn's disease patients hierarchical and leaning performance. A: Heatmap of the 9-selected miRNA intensity. Colour corresponding to the status of the patients: Purple: green: Cases and yellow: Controls; B: Receiver operating characteristic curve for the classification using random forests analysis; C: Using L-SVM models for the 9 selected miRNA. AUC: Area under the curve.

The local signature of UC patients

To identify a significant signature of UC patients we analysed a data set of 121 individuals. These patients are distributed in 42 cases and 79 controls respectively. Upon applying the previous approach to these samples, a signature of 30 miRNAs differentially expressed between cases and control in UC

was detected. The results derived from this calculation are plotted below in [Figure 4](#).

As occurred with the two previous results, see [Figure 2](#) and [Figure 3](#), the presence of data heterogeneity hampers a right classification of patients when using the Euclidean norm across the expression profile of the detected 30 miRNAs. Additionally, the classification results yielded by the two learning methods used in this work are displayed by their ROC curves in [Figure 4B](#) and [C](#). These curves attain a sensitivity-specificity ranges of 0.45-0.86 and 0.55-0.87 to RF and SVM respectively. And the miRNAs selected by multiple comparison of the annotated miRNAs achieved a percentage of success in classification of 76% across the mean expression of each group of patients. These amounts are slightly lower than in CD patients. Such a drop can be explained by a more scatter matching distribution among UC patients as well as a greater control-case ratio. The confusion matrix corresponding to this calculation is introduced above in [Table 5](#).

Minimising the size of the overall signature by parse PLS discriminant analysis

Despite the relative low size of the prognostic signature identified so far, we wonder if it was possible to minimise the amount of miRNAs involved in the analysis without harming the overall classification performance. The statistical robustness of the parse PLS Discriminant Analysis in supervised feature selection makes us to consider its application before performing the unsupervised hierarchical clustering introduced in methods. The stratification of all patients is plotted in [Figure 5A](#) while [Figure 5B](#) describes the diseases tree architecture. The synergy between the two complementary statistical methods, supervised later unsupervised, still allow us to conclude the predictive power of the miRNAs minimal signature associated with CRC in IBD.

Reconstructing the overall signature: After having applied the proposed sPLS-DA to the miRNAs, the reconstruction of the tree structure based on the multi-class comparison strategy 1 improved the previous classification of patients between clusters ([Figure 5B](#)). The analysis of patients following such architecture resulted in a final signature composed by 11 miRNAs. Hence, these selected miRNAs correctly classified the 69% and 68% of cases (RF and SVM respectively). Both percentages are similar in accuracy to those obtained without the use of sPLS-DA, but with a signature consisting of only 11 out of initial 56 miRNAs. Nevertheless, the effect of the genetic drift of CD and UC origin could not have been prevented. We also provide the overall performance of the methods as a confusion matrix in the [Table 6](#). For further details on the variable importance of this signature in the RF calculation see supplemental information ([Supplementary Figure 9A](#)).

Reconstructing the local signature of the CD patients: In this analysis 5 miRNAs were selected with the recursion cluster for CD patients. The SVM allows a better classification of true patients in the 82% of cases, and particularly the controls patients. The RF and SVM performances along their feature selection refining are presented in [Figure 6B](#). See supplemental material for details on variable importance for each miRNA ([Supplementary Figure 9B](#)) of the RF computation. We also obtain their patients classification in a confusion matrix presented in [Table 7](#). The accuracy and sensitivity are consistent with the above percentage of classification in CD patients reducing the signature in 4 miRNAs up to a final figure of 5 predictive profiles.

Reconstructing the local signature of UC patients: The overall signature of UC patients after making use of sPLS-DA was composed of 8 miRNAs. We also calibrated models by feature selection of these miRNAs, which results are shown in the [Figure 6C](#). The attained percentage of success goes to the 81% upon computation of a SVM model across UC samples what improved the RF performance as had already occurred with previous counterpart calculations. For further details on the RF analysis see [Supplementary Figure 9C](#). Strikingly the use of sPLS-DA enabled reducing the quantity of miRNAs required to predict UC patients developing or not CRC from 30 to 8 while increasing in a 5% the percentage of success. This may be due to the detection and later removal of features largely contributing to the dispersal form of the matching distribution among UC patients. Finally, the confusion matrix corresponding to this miRNAs signature is described below in [Table 8](#).

DISCUSSION

The soundness of the signature has been improved accordingly to the incremental combination of learning methods presented in this study until attain a sensitivity of 73% in CD and 57% in UC with a specificity of 87% and 93% in CD and UC respectively (see [Table 2](#)). These results are depending on the assumption of an initial hierarchical tree structure. The usage of PLS-DA decreases a bit its global sensitivity but gaining more in CRC signature optimisation. Noteworthy, the final overall signature is composed by only 5 miRNAs in CD and 8 in UC. These miRNAs are molecules extremely resistant and highly preserved. In general, low percentages of true classification are obtained is no difference on disease type is made on the IBD patients. This is in accordance with previous works that suggest the genetic divergence between CD and UC. However, if we consider the two types of the disease separately, the aim of classifying false controls, i.e., controls with a closer profile to cases and

Table 5 Contingence matrix of the 30-selected miRNA and random forests methods for Ulcerative colitis patients

Predicted by RF		Predicted by SVM			
		Cases	Controls	Cases	Controls
True	Case	19	23	23	19
	Controls	11	68	10	69

RF: Random forests; SVM: Support vector machines.

Table 6 Contingence matrix of the 11-selected miRNA and random forests methods for all patients

Predicted by RF		Predicted by SVM			
		Cases	Controls	Cases	Controls
True	Case	27	45	26	46
	Controls	18	116	19	115

RF: Random forests; SVM: Support vector machines.

Table 7 Contingence matrix of the 5-selected miRNA and random forests methods for Crohn's disease patients

Predicted by RF		Predicted by SVM			
		Cases	Controls	Cases	Controls
True	Case	20	10	20	10
	Controls	7	48	5	50

RF: Random forests; SVM: Support vector machines.

Table 8 Contingence matrix of the 9-selected miRNA and random forests methods for Ulcerative colitis patients.

Predicted by RF		Predicted by SVM			
		Cases	Controls	Cases	Controls
True	Case	20	22	24	18
	Controls	11	68	5	74

RF: Random forests; SVM: Support vector machines.

monitoring whether those samples are developing cancer can be approached now. Indeed, the introduced methodology would allow us to provide the identified molecular signature with predictive power. Additionally, the eventual availability of a second independent cohort could improve possibly the precision of results. Thus, we claim that in any case a clinician having this information will potentially benefit from an accurate prediction tool of prognosis rather than only using his or her own experience-based criteria[30,31]. This clinical scenario enhances the paramount importance of statistical learning-based applications in clinical practice since CRC is a feared life-threatening factor among patients with IBD[32,33]. In particular, the analysis of eventual miRNAs signatures associated with CRC in patients with IBD has been successfully proven previously in such contexts[34-36]. That way, these methodologies will contribute to shorten unnecessary delays prior to make any decision on a proper therapy in individuals with a IBD developing CRC[37,38].

CONCLUSION

In this study we provide a wise combination of statistical learning methods for patients' stratification

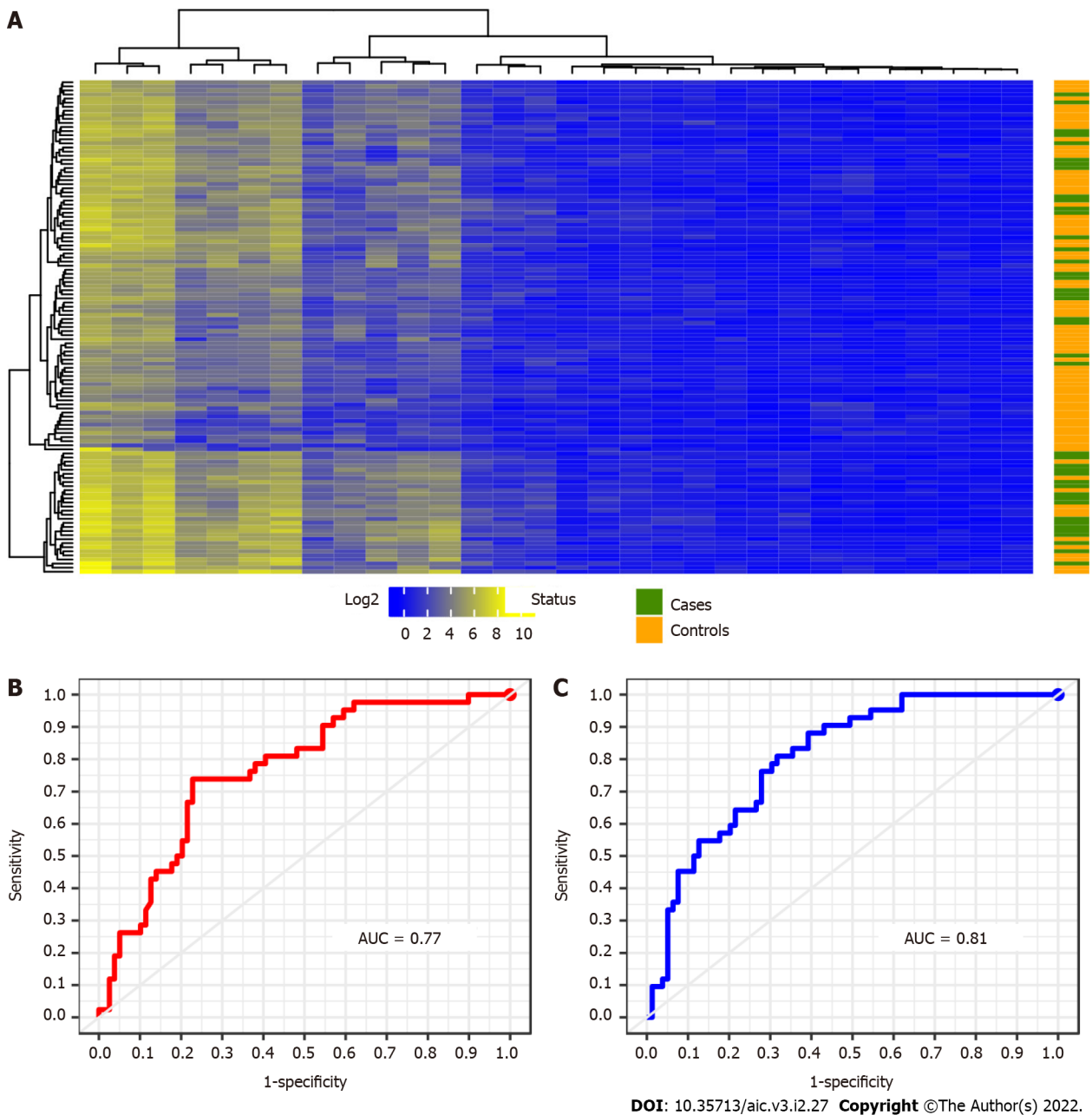


Figure 4 Ulcerative colitis patients hierarchical and leaning performance. A: Heatmap of the 30-selected miRNA intensity. Colour corresponding to the status of the patients: Purple: Green: Cases and yellow: Controls; B: Receiver operating characteristic curve for the classification using random forests analysis; C: Using L-SVM models for the 30-selected miRNA. AUC: Area under the curve.

based on biologically meaningful characteristics, and its application in IBD based on a minimal miRNA network associated with CRC is demonstrated. The time constraint affecting the assessment of the response to the medical treatment indicates the interest of our method in improving the classification accuracy, minimising the signature of miRNAs required in the IBD patients' stratification, and avoiding unnecessary time delays. The findings are also consistent with the physio-pathological knowledge. Comparison with other existing classifying method shows that SVM makes our method yields better mean performances, using a reduced miRNA signature and reporting a much lower sensitivity to data heterogeneity. The application of the proposed method to a multi-class classification further points out the robustness and efficiency of our strategy particularly in the CD and UC group of patients. Additionally, the use of parse PLS Discriminant Analysis is also concluded for a minimal signature with accurate enough performances. In the next future, we will combine this method with other approaches such as deep learning methods enabling more intricate relationships between the elements of the signature and possibly another robust clinical data. Finally, we are convinced our methodology will be also instrumental for other diseases broadening the general framework herein provided.

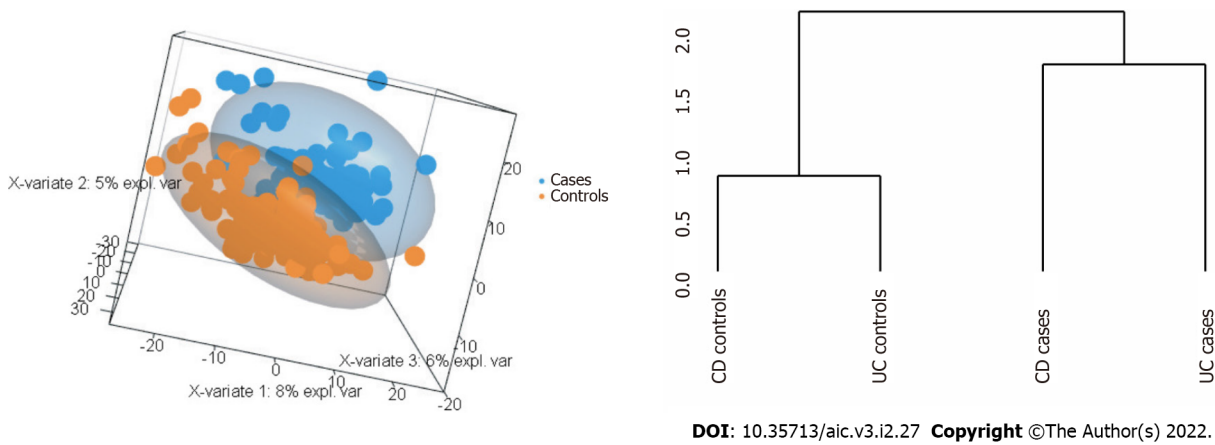


Figure 5 Partial least squares discriminant analysis base. Left-hand side panel: Patient-control stratification (*i.e.* orange-blue) in three dimensional view with 152 miRNAs; Right-hand side panel: Classification tree with the 152 miRNAs selected by sPLS-DA.

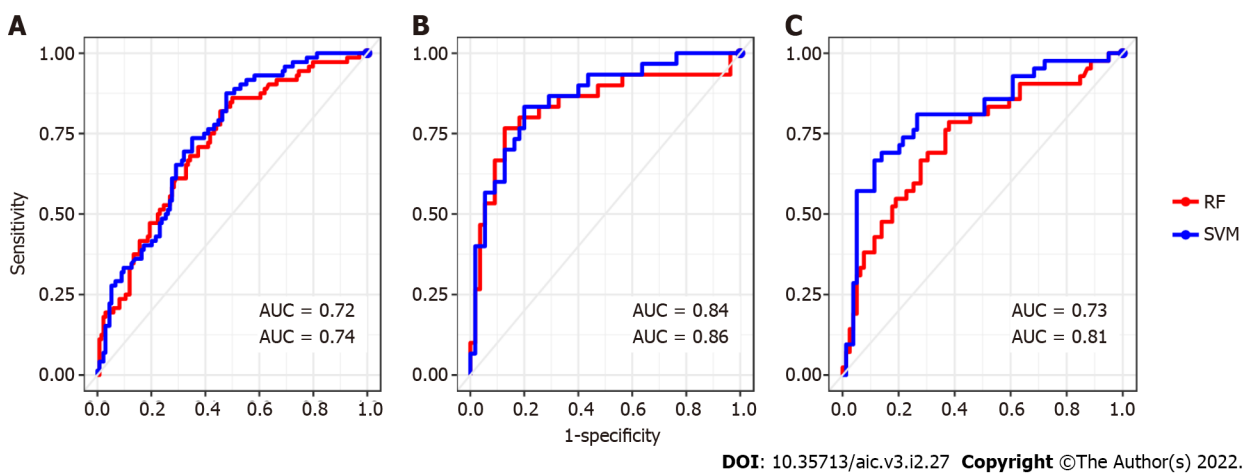


Figure 6 Final performance of each reconstructed sub-signature. A: Receiver operating characteristic curve amounts to all patients learned classification by a signature corresponding to 13 selected miRNA; B: Similarly to the Crohn’s disease patients classification of 5 selected miRNA; C: Ulcerative colitis patients classified according to 9 selected miRNA.

ARTICLE HIGHLIGHTS

Research background

Face the overabundance of information, it is not easy to clinicians discriminating amid biological indicators that potentially could be helpful during an inflammatory bowel disease (IBD) disease therapy.

Research motivation

There exist intra patient differences in miRNA expression between the inflammatory and healthy tissue, between the healthy tissue of an inflammatory and non-inflammatory patient and between the healthy tissue of a cancer and non- cancer colic patient. We want to identify a minimal miRNA profile of developing or not cancer in patients with a chronic inflammatory bowel disease. In other words, a miRNA profile of healthy tissue from patients with chronic IBD with (case) *vs* without cancer (control). In that way, provided a specific miRNA profile is of interest, this one could be prospectively validated, and its predictive marker maybe also developed. Ultimately, this would allow clinicians to increase the diagnosis colonoscopy pace in IBD patients where a miRNA profile of risk is detected and conversely decreasing that pace in patients tagged as at lower risk.

Research objectives

In this scenario, the identification of an optimal signature, for example composed by microRNA (miRNA), associated with colorectal cancer (CRC) in patients with one chronic IBD is of vital importance.

Research methods

We provide a framework of well-established statistical learning methods (*i.e.*, RF, SVM, PLS-DA, ...) wisely adapted to reconstructing a CRC network leveraged to stratify these patients.

Research results

Our strategy provides an adjusted signature of 5 miRNAs with a percentage of success in patient classification of 82% in Crohn's disease (resp. 81% in Ulcerative Colitis).

Research conclusions

The application of the proposed method to a multi-class classification further points out the robustness and efficiency of our strategy particularly in the CD and UC group of patients. Additionally, the use of sparse PLS Discriminant Analysis spots a minimal signature with accurate enough performances.

Research perspectives

In the next future, the combination of this method with deep learning models will enable more intricate relationships between the elements of the signature and possibly another robust clinical data. Finally, we are convinced our methodology will be also instrumental for other diseases broadening the general framework herein provided.

FOOTNOTES

Author contributions: Morilla I conceived and designed the computational experiments; Abaach M and Morilla I performed computational experiments, analyzed the miRNomic data, performed formal analysis; Morilla I wrote the original manuscript Abaach M and Morilla I reviewed and edited the manuscript.

Institutional review board statement: The protocols involving human participants conformed to the local Ethics Committee (CPP-Île de France IV No. 2009/17) and to the principles set out in the WMA Declaration of Helsinki, and the Belmont Report from the Department of Health and Human Services. Human ileal biopsies were obtained from the IBD Gastroenterology Unit, Beaujon Hospital and a written informed consent was obtained from all the patients before inclusion in the study.

Institutional animal care and use committee statement: The protocols involving human participants conformed to the local Ethics Committee (CPP-Île de France IV No. 2009/17) and to the principles set out in the WMA Declaration of Helsinki, and the Belmont Report from the Department of Health and Human Services. Human ileal biopsies were obtained from the IBD Gastroenterology Unit, Beaujon Hospital and a written informed consent was obtained from all the patients before inclusion in the study.

Conflict-of-interest statement: All authors declare no conflicts of interest in this paper.

Data sharing statement: The R code for implementing the inference procedures is available at <https://figshare.com/account/home#/projects/36290>. The results of the inference, along with instructions on how to use these files to recreate the figures in this paper, are available at <https://figshare.com/account/home#/projects/36290/>.

ARRIVE guidelines statement: The authors have read the ARRIVE guidelines, and the manuscript was prepared and revised according to the ARRIVE guidelines.

Open-Access: This article is an open-access article that was selected by an in-house editor and fully peer-reviewed by external reviewers. It is distributed in accordance with the Creative Commons Attribution NonCommercial (CC BY-NC 4.0) license, which permits others to distribute, remix, adapt, build upon this work non-commercially, and license their derivative works on different terms, provided the original work is properly cited and the use is non-commercial. See: <https://creativecommons.org/licenses/by-nc/4.0/>

Country/Territory of origin: France

ORCID number: Mariem Abaach [0000-0001-6855-7014](https://orcid.org/0000-0001-6855-7014); Ian Morilla [0000-0002-5100-5990](https://orcid.org/0000-0002-5100-5990).

Corresponding Author's Membership in Professional Societies: Université Sorbonne Paris Nord.

S-Editor: Liu JH

L-Editor: A

P-Editor: Liu JH

REFERENCES

- 1 **Goodwin S**, McPherson JD, McCombie WR. Coming of age: ten years of next-generation sequencing technologies. *Nat Rev Genet* 2016; **17**: 333-351 [PMID: 27184599 DOI: 10.1038/nrg.2016.49]
- 2 **Morilla I**, Lees JG, Reid AJ, Orengo C, Ranea JA. Assessment of protein domain fusions in human protein interaction networks prediction: application to the human kinetochore model. *N Biotechnol* 2010; **27**: 755-765 [PMID: 20851221 DOI: 10.1016/j.nbt.2010.09.005]
- 3 **Morilla I**, Doblas S, Garteiser P, Zappa M, Ogier-Denis E. Scores of intestinal fibrosis from wavelet-based magnetic resonance imaging models. Rojas I, Ortuño F, editors. *Bioinformatics and Biomedical Engineering* (Springer International Publishing), 2017: 569-578 [DOI: 10.1007/978-3-319-56148-6_51]
- 4 **Ng SC**, Shi HY, Hamidi N, Underwood FE, Tang W, Benchimol EI, Panaccione R, Ghosh S, Wu JCY, Chan FKL, Sung JY, Kaplan GG. Worldwide incidence and prevalence of inflammatory bowel disease in the 21st century: a systematic review of population-based studies. *Lancet* 2017; **390**: 2769-2778 [PMID: 29050646 DOI: 10.1016/S0140-6736(17)32448-0]
- 5 **Morilla I**, Uzzan M, Laharie D, Cazals-Hatem D, Denost Q, Daniel F, Belleanne G, Bouhnik Y, Wainrib G, Panis Y, Ogier-Denis E, Treton X. Colonic MicroRNA Profiles, Identified by a Deep Learning Algorithm, That Predict Responses to Therapy of Patients With Acute Severe Ulcerative Colitis. *Clin Gastroenterol Hepatol* 2019; **17**: 905-913 [PMID: 30223112 DOI: 10.1016/j.cgh.2018.08.0688]
- 6 **Sedghi S**, Barreau F, Morilla I, Montcuquet N, Cazals-Hatem D, Pedruzzi E, Rannou E, Tréton X, Hugot JP, Ogier-Denis E, Daniel F. Increased Proliferation of the Ileal Epithelium as a Remote Effect of Ulcerative Colitis. *Inflamm Bowel Dis* 2016; **22**: 2369-2381 [PMID: 27598740 DOI: 10.1097/MIB.0000000000000871]
- 7 **Kim ER**, Chang DK. Colorectal cancer in inflammatory bowel disease: the risk, pathogenesis, prevention and diagnosis. *World J Gastroenterol* 2014; **20**: 9872-9881 [PMID: 25110418 DOI: 10.3748/wjg.v20.i29.9872]
- 8 **Mattar MC**, Lough D, Pishvaian MJ, Charabaty A. Current management of inflammatory bowel disease and colorectal cancer. *Gastrointest Cancer Res* 2011; **4**: 53-61 [PMID: 21673876 DOI: 10.1007/s11888-010-0061-2]
- 9 **Wang Y**, LêCao KA. Managing batch effects in microbiome data. *Brief Bioinform* 2020; **21**: 1954-1970 [PMID: 31776547 DOI: 10.1093/bib/bbz105]
- 10 **Breiman L**. Random forests. *Machine Learning*, 2001: 5-32 ISSN 1573-0565 [DOI: 10.1023/a:1010933404324]
- 11 **F Wenzel**, T Galy-Fajou, M Deutsch, and M Kloft. Bayesian nonlinear support vector machines for big data. In *ECML/PKDD*, pages 10–20, 2017. [DOI: 10.1007/978-3-319-71249-9_19]
- 12 **Vapnik VN**. *The Nature of Statistical Learning Theory*. Springer: New York, USA, 1995 [DOI: 10.1007/978-1-4757-2440-0]
- 13 **Arlot S**, Celisse A. A survey of cross-validation procedures for model selection. *Statistics Surveys* 2010; **4**: 40-79 [DOI: 10.1214/09-ss054]
- 14 **Sokolova M**, Lapalme G. A systematic analysis of performance measures for classification tasks. *Information Processing and Management* 2009; **45**: 427-437 [DOI: 10.1016/j.ipm.2009.03.002]
- 15 **Gomes P**, du Boulay C, Smith CL, Holdstock G. Relationship between disease activity indices and colonoscopic findings in patients with colonic inflammatory bowel disease. *Gut* 1986; **27**: 92-95 [PMID: 3949241 DOI: 10.1136/gut.27.1.92]
- 16 **Mosli MH**, Feagan BG, Sandborn WJ, D'haens G, Behling C, Kaplan K, Driman DK, Shackleton LM, Baker KA, Macdonald JK, Vandervoort MK, Geboes K, Levesque BG. Histologic evaluation of ulcerative colitis: a systematic review of disease activity indices. *Inflamm Bowel Dis* 2014; **20**: 564-575 [PMID: 24412993 DOI: 10.1097/01.MIB.0000437986.00190.71]
- 17 **Bumgarner R**. Overview of DNA microarrays: types, applications, and their future. *Curr Protoc Mol Biol* 2013; **Chapter 22**: Unit 22.1. [PMID: 23288464 DOI: 10.1002/0471142727.mb2201s101]
- 18 **Jolliffe IT**. *Principal Component Analysis*. 2nd ed. Springer-Verlag, 2002 [DOI: 10.1007/978-1-4757-1904-8_7]
- 19 **Gan L**, Denecke B. Profiling Pre-MicroRNA and Mature MicroRNA Expressions Using a Single Microarray and Avoiding Separate Sample Preparation. *Microarrays (Basel)* 2013; **2**: 24-33 [PMID: 27605179 DOI: 10.3390/microarrays2010024]
- 20 **Smyth GK**. Linear models and empirical bayes methods for assessing differential expression in microarray experiments. *Stat Appl Genet Mol Biol* 2004; **3**: Article3 [PMID: 16646809 DOI: 10.2202/1544-6115.1027]
- 21 **Rice JA**. *Mathematical Statistics and Data Analysis*. 2nd ed. Wadsworth Publishing Co Inc, 1994 [DOI: 10.1016/0167-9473(94)90164-3]
- 22 **Barker M**, Rayens W. Partial least squares for discrimination. *Journal of Chemometrics* 2003; **17**: 166-73 [DOI: 10.1002/cem.785]
- 23 **Rohart F**, Gautier B, Singh A, Lê Cao KA. mixOmics: An R package for 'omics feature selection and multiple data integration. *PLoS Comput Biol* 2017; **13**: e1005752 [PMID: 29099853 DOI: 10.1371/journal.pcbi.1005752]
- 24 **Melkumova LE**, Shatskikh SY. Comparing Ridge and LASSO estimators for data analysis. *Procedia Engineering* 2017; **201**: 746-755 [DOI: 10.1016/j.proeng.2017.09.615]
- 25 **A Statnikov**, D Hardin, and C Aliferis. Using SVM weight-based methods to identify causally relevant and non-causally relevant variables. *Sign*, 1(4):474-484, 2006. [DOI: 10.1037/dev0000872.supp]
- 26 **Liaw A**, Wiener M. Classification and regression by randomforest. R News. 2002. Available from https://www.r-project.org/doc/Rnews/Rnews_2002-3.pdf
- 27 **Wei P**, Lu Z, Song J. Variable importance analysis: A comprehensive review. *Reliability Engineering and System Safety* 2015; **142**: 399-432 [DOI: 10.1016/j.res.2015.05.018]
- 28 **Kuhn M**. Building predictive models in r using the caret package. *Journal of statistical software* 2008; **5**: 1-26 [DOI: 10.18637/jss.v028.i05]
- 29 **Sachs MC**. plotROC: A Tool for Plotting ROC Curves. *J Stat Softw* 2017; **79** [PMID: 30686944 DOI: 10.18637/jss.v079.c02]
- 30 **Damião AOMC**, de Azevedo MFC, Carlos AS, Wada MY, Silva TVM, Feitosa FC. Conventional therapy for moderate to severe inflammatory bowel disease: A systematic literature review. *World J Gastroenterol* 2019; **25**: 1142-1157 [PMID: 31776547 DOI: 10.1093/bib/bbz105]

- 30863001 DOI: [10.3748/wjg.v25.i9.1142](https://doi.org/10.3748/wjg.v25.i9.1142)]
- 31 **Cross RK**, Farraye FA. IBD management: Stat of the art in 2018. *Gastroenterology & Hepatology* 2018; **11**: 6 [DOI: [10.1111/jgh.14395](https://doi.org/10.1111/jgh.14395)]
 - 32 **Lucafò M**, Curci D, Franzin M, Decorti G, Stocco G. Inflammatory Bowel Disease and Risk of Colorectal Cancer: An Overview From Pathophysiology to Pharmacological Prevention. *Front Pharmacol* 2021; **12**: 772101 [PMID: [34744751](https://pubmed.ncbi.nlm.nih.gov/34744751/) DOI: [10.3389/fphar.2021.772101](https://doi.org/10.3389/fphar.2021.772101)]
 - 33 **Ishimaru K**, Tominaga T, Nonaka T, Fukuda A, Moriyama M, Oyama S, Ishii M, Sawai T, Nagayasu T. Colorectal cancer in Crohn's disease: a series of 6 cases. *Surg Case Rep* 2021; **7**: 152 [PMID: [34181132](https://pubmed.ncbi.nlm.nih.gov/34181132/) DOI: [10.1186/s40792-021-01237-0](https://doi.org/10.1186/s40792-021-01237-0)]
 - 34 **Grillo TG**, Quaglio AEV, Beraldo RF, Lima TB, Baima JP, Di Stasi LC, Sasaki LY. MicroRNA expression in inflammatory bowel disease-associated colorectal cancer. *World J Gastrointest Oncol* 2021; **13**: 995-1016 [PMID: [34616508](https://pubmed.ncbi.nlm.nih.gov/34616508/) DOI: [10.4251/wjgo.v13.i9.995](https://doi.org/10.4251/wjgo.v13.i9.995)]
 - 35 **Yu M**, Luo Y, Cong Z, Mu Y, Qiu Y, Zhong M. MicroRNA-590-5p Inhibits Intestinal Inflammation by Targeting YAP. *J Crohns Colitis* 2018; **12**: 993-1004 [PMID: [29912317](https://pubmed.ncbi.nlm.nih.gov/29912317/) DOI: [10.1093/ecco-jcc/jjy046](https://doi.org/10.1093/ecco-jcc/jjy046)]
 - 36 **Bocchetti M**, Ferraro MG, Ricciardiello F, Ottaiano A, Luce A, Cossu AM, Scrima M, Leung WY, Abate M, Stiuso P, Caraglia M, Zappavigna S, Yau TO. The Role of microRNAs in Development of Colitis-Associated Colorectal Cancer. *Int J Mol Sci* 2021; **22** [PMID: [33921348](https://pubmed.ncbi.nlm.nih.gov/33921348/) DOI: [10.3390/ijms22083967](https://doi.org/10.3390/ijms22083967)]
 - 37 **Vogel JD**, Eskicioglu C, Weiser MR, Feingold DL, Steele SR. The American Society of Colon and Rectal Surgeons Clinical Practice Guidelines for the Treatment of Colon Cancer. *Dis Colon Rectum* 2017; **60**: 999-1017 [PMID: [28891842](https://pubmed.ncbi.nlm.nih.gov/28891842/) DOI: [10.1097/DCR.0000000000000926](https://doi.org/10.1097/DCR.0000000000000926)]
 - 38 **Luzietti E**, Pellino G, Nikolaou S, Qiu S, Mills S, Warren O, Tekkis P, Kontovounisios C. Comparison of guidelines for the management of rectal cancer. *BJS Open* 2018; **2**: 433-451 [PMID: [30511044](https://pubmed.ncbi.nlm.nih.gov/30511044/) DOI: [10.1002/bjs5.88](https://doi.org/10.1002/bjs5.88)]



Published by **Baishideng Publishing Group Inc**
7041 Koll Center Parkway, Suite 160, Pleasanton, CA 94566, USA
Telephone: +1-925-3991568
E-mail: bpgoffice@wjgnet.com
Help Desk: <https://www.f6publishing.com/helpdesk>
<https://www.wjgnet.com>

